W/Z bremsstrahlung as the dominant annihilation channel for dark matter

Nicole F. Bell, James B. Dent, Thomas D. Jacques, and Thomas J. Weiler

Phys. Rev. D **83**, 013001 — Published 6 January 2011

DOI: 10.1103/PhysRevD.83.013001

W/Z Bremsstrahlung as the Dominant Annihilation Channel for Dark Matter

Nicole F. Bell,[1] James B. Dent,[2] Thomas D. Jacques,[1] and Thomas J. Weiler[3]

[1]*School of Physics, The University of Melbourne, Victoria 3010, Australia*
[2]*Department of Physics and School of Earth and Space Exploration, Arizona State University, Tempe, AZ 85287-1404, USA*
[3]*Department of Physics and Astronomy, Vanderbilt University, Nashville, TN 37235, USA*

Dark matter annihilation to leptons, $\chi\chi \to \ell\bar{\ell}$, is necessarily accompanied by electroweak radiative corrections, in which a W or Z boson is radiated from a final state particle. Given that the W and Z gauge bosons decay dominantly via hadronic channels, it is thus impossible to produce final state leptons without accompanying protons, antiprotons, and gamma rays. Significantly, while many dark matter models feature a helicity suppressed annihilation rate to fermions, radiating a massive gauge boson from a final state fermion removes this helicity suppression, such that the branching ratios Br($\ell\nu W$), Br($\ell^+\ell^- Z$), and Br($\nu\bar{\nu}Z$) dominate over Br($\ell\bar{\ell}$). W/Z-bremsstrahlung thus allows indirect detection of many WIMP models that would otherwise be helicity-suppressed, or v^2 suppressed. Antiprotons and even anti-deuterons become consequential final state particles. This is an important result for future DM searches. We discuss the implications of W/Z-bremsstrahlung for "leptonic" DM models which aim to fit recent cosmic ray positron and antiproton data.

PACS numbers: 95.35.+d, 12.15.Lk, 95.85.Ry

I. INTRODUCTION

An abundance of cosmological and astrophysical evidence attests to the existence of dark matter (DM), whose presence is inferred via its gravitational influence [1–3]. However, the fundamental particle properties of DM remain essentially unknown. One important means of probing DM's particle nature is via indirect detection, whereby we search for products of DM annihilation (or decay) emanating from regions of DM concentration in the Universe today.

The dark matter annihilation cross section is often parametrized as $\langle v\sigma_A\rangle = a + bv^2 + \cdots$, where $\langle v\sigma_A\rangle$ is the thermally-averaged annihilation cross section. The constant a comes from s-wave annihilation, while the velocity suppressed bv^2 term receives both s-wave and p-wave contributions; the L^{th} partial wave contribution to the annihilation rate is suppressed as v^{2L}. Given that $v \sim 10^{-3}c$ in galactic halos, even the p-wave contribution is highly suppressed and thus only the s-wave contribution is expected to be significant in the Universe today. However, in many DM models the s-wave annihilation into a fermion pair $\chi\chi \to \bar{f}f$ is helicity suppressed by a factor $(m_f/M_\chi)^2$ (only $\to \bar{t}t$ modes remain of interest, and then only for a certain range of χ mass).

When computing DM annihilation signals, it is normally assumed that only the lowest order tree-level processes make a significant contribution. However, there are important exceptions to this statement. Dark matter annihilation into charged particles, $\chi\chi \to \bar{f}f$, is necessarily accompanied by the internal bremsstrahlung process $\chi\chi \to \bar{f}f\gamma$, where the photon may be radiated from one of the external particle legs (final state radiation, FSR) or, possibly, from a virtual propagator (virtual internal bremsstrahlung, VIB). On the face of it, the radiative rate is down by the usual QED coupling factor of $\alpha/\pi \sim 500$. However, and significantly, photon bremsstrahlung can lift the helicity suppression of the s-wave process [4], which more than compensates for the extra coupling factor. Such a striking enhancement can arise when a symmetry of the initial state $\chi\chi$ is satisfied by the three body final state $\bar{f}f\gamma$, but not by the two body final state $\bar{f}f$. For bremsstrahlung of photons, only VIB is effective in lifting the helicity suppression, as FSR is dominated by soft or collinear photons (such that the two and three body final states have the same symmetry properties) as discussed in Ref. [5].

In this paper we examine electroweak bremsstrahlung [6–11], i.e., bremsstrahlung of Z or $W^\pm$ electroweak gauge bosons to produce $\bar{f}fZ$ and $\bar{\ell}\nu W$ final states. The virtue for W/Z bremsstrahlung to lift initial-state velocity and final-state helicity suppressions, alluded to in [8, 11], has not been previously explored. We show that W/Z-bremsstrahlung can also lift suppression and become the dominant annihilation channel. Thus, W/Z bremsstrahlung allows indirect detection of many WIMP models that would otherwise be helicity-suppressed, or v^2 suppressed. This is an important result for future DM searches.

There are a number of important distinctions between electromagnetic (EM) and electroweak (EW) bremsstrahlung. An obvious one is that EM bremsstrahlung produces just photons, whereas EW bremsstrahlung and subsequent decay of the gauge bosons leads to leptons, hadrons and gamma rays, offering correlated "multi-messenger" signals for indirect dark matter searches. Another distinction is that W/Z-bremsstrahlung from final state particles (FSR) is sufficient to lift a suppression. This is due to the nonzero gauge boson masses, and the coupling of the gauge bosons to the non-conserved axial current which leads to a different form for the polarization sum than in the case of the photon (or a gluon in the similar QCD process). In contrast, for the EM process, VIB is required for the photon to lift a suppression. Because an additional propagator appears for VIB, suppression-lifting EM bremsstrahlung is itself suppressed by an additional factor of M_χ^2/M_η^2 relative to electroweak's FSR, where M_η is the mass of the internal exchange-particle. Only in the event of a near-degeneracy $M_\chi \sim M_\eta$ is this relative suppression of EM bremsstrahlung negligible.

DM annihilation to charged leptons has been the subject of much recent attention, due to recently measured cosmic ray anomalies which point to an excess of cosmic ray positrons above those that may be attributed to conventional astrophysical processes. PAMELA has observed a sharp excess in the $e^+/(e^-+e^+)$ fraction at energies beyond approximately 10 GeV [12], without a corresponding excess in the antiproton/proton data [13, 14], while Fermi and HESS have reported more modest excesses in the (e^-+e^+) flux at energies of order 1 TeV [15]. These signals have led to a re-examination of positron production in nearby pulsars [16], emission from supernova remnants [17], acceleration of e^+e^- in cosmic ray sources [18], and propagation in conventional cosmic ray models [19]. As an alternative to these astrophysical mechanisms, it has also been proposed that the excess e^+ and e^- are produced via dark matter annihilation in the Galactic halo, with an abundance of DM models proposed to accomplish this end. A recent overview of $e^\pm$-excess data and possible interpretations is available in [20].

However, some of the most popular models suffer from helicity or v^2-suppression. A prototypical example of suppressed production of Standard Model (SM) fermion pairs is provided by supersymmetry: Majorana neutralinos annihilate into a pair of SM fermions via t- and u-channel exchange of $SU(2)$-doublet sfermions. To overcome the suppression, proponents of these models have invoked large "boost" factors. These boost factors may be astrophysical in origin, as with postulated local overdensities of dark matter, or they may arise from particle physics, as with the Sommerfeld enhancement that arises from light scalar exchange between dark matter particles. Although not ruled out, these factors do seem to be a contrivance designed to overcome the innate suppression.

A further problem with suppressed models is the overproduction of antiprotons from unsuppressed W/Z bremsstrahlung. Given that hadronic decay modes of the W and Z bosons will lead to significant numbers of both antiprotons and gamma rays, this will impact the viability of models that might otherwise have explained the observed positron excess. Even in models which do not feature a suppression, the W/Z-bremsstrahlung has important phenomenological consequences, as the decay products of the gauge bosons make a pure leptonic e^+e^- signal impossible [11].

In Section II we discuss the circumstances under which dark matter annihilation may be suppressed, and in Section III explain how W/Z bremsstrahlung is able to circumvent such a suppression. In Section IV we consider a representative model, and explicitly calculate the cross sections for both the lowest order annihilation process, and for the W/Z bremsstrahlung process. We discuss implications of these results in Section V. Calculational details are collected in five Appendices.

II. UNDERSTANDING SUPPRESSION USING FIERZ TRANSFORMATIONS

In this section we describe the origin of v^2 and helicity suppressions. We shall make use of Fierz transformation and partial wave decomposition to determine under what circumstances these suppressions will or will not arise.

Dark matter candidates may be scalar, fermionic, or vector in nature; if fermionic, they may be either Dirac or Majorana. Permissible annihilation models include s-, t-, and u-channel exchanges of a new particle, and the various possibilities are listed in Refs. [21–23]. In every case, it is useful to classify the partial waves available to the decay process, and to analyze the dependence on the mass of the SM particle-pair in the final state. In this article, we focus on fermionic Majorana dark matter.

For fermionic dark matter, the natural projection of $2 \to 2$ processes into partial waves makes use of the Fierz transformation. In the next subsection we consider DM annihilation via the process $\chi\chi \to \bar{f}f$, and explain the use of Fierz transforms to convert the matrix elements for t/u-channel annihilation, which are of the form $(\overline{\chi}\,\Gamma_A l)(\bar{l}\,\Gamma_B\chi)$, to a sum of s-channel amplitudes of the form $(\overline{\chi}\,\Gamma_1\chi)(\bar{l}\,\Gamma_2 l)$. In the following subsection we then categorize the Fierzed s-channel amplitudes into partial waves and fermion-pair spin states, which determines whether the amplitudes are velocity suppressed, mass-suppressed, or unsuppressed. In the third and final subsection, we put our findings together to determine which class of models will have a suppressed $2 \to 2$ annihilation. We show that in a certain popular class of suppressed models, the $2 \to 3$ W/Z-bremsstrahlung process is unsuppressed, and in fact dominant for $2\,M_\chi > M_W$. We will find in Section III that a generalization of the Fierz transformation offers useful insight into the non-suppression of the $2 \to 3$ process.

A. Fierz Transformations in the Chiral Basis

Helicity projection operators are essential in chiral gauge theories, so it is worth considering the reformulation of Fierz transformations in the chiral basis [24]. (A discussion of standard Fierz transformations may be found in, e.g. Ref. [25].) We place hats above the generalized Dirac matrices constituting the chiral basis. These matrices are

$$\{\hat{\Gamma}^B\} = \{P_R,\, P_L,\, P_R\gamma^\mu,\, P_L\gamma^\mu,\, \frac{1}{2}\sigma^{\mu\nu}\}\,, \quad \text{and}$$
$$\{\hat{\Gamma}_B\} = \{P_R,\, P_L,\, P_L\gamma_\mu,\, P_R\gamma_\mu,\, \frac{1}{2}\,\sigma_{\mu\nu}\}\,, \qquad (1)$$

where $P_R \equiv \frac{1}{2}(1+\gamma_5)$ and $P_L \equiv \frac{1}{2}(1-\gamma_5)$ are the usual helicity projectors. Notice that the dual of $P_R\gamma^\mu$ is $P_L\gamma_\mu$, and the dual of $P_L\gamma^\mu$ is $P_R\gamma_\mu$. The tensor matrices in this basis contain factors of $\frac{1}{2}$: $\hat{\Gamma}^T = \frac{1}{2}\sigma^{\mu\nu}$ and $\hat{\Gamma}_T = \frac{1}{2}\sigma_{\mu\nu}$. These facts result from the orthogonality and normalization properties of the chiral basis and its dual, as explained in detail in Appendix A.

Using completeness of the basis (see Appendix A), one arrives at a master formula which expands the outer product of two chiral matrices in terms of their Fierzed forms:

$$(\hat{\Gamma}^D)\,[\hat{\Gamma}_E] = \frac{1}{4}\,Tr\,[\hat{\Gamma}^D\,\hat{\Gamma}^C\,\hat{\Gamma}_E\,\hat{\Gamma}_B]\;(\hat{\Gamma}^B]\,[\hat{\Gamma}_C)\,, \tag{2}$$

where the parentheses symbols are a convenient shorthand for matrix indices [26] (see the appendix for details). Evaluating the trace in Eq. (2) leads to the Fierz transformation matrix in the chiral-basis:

$$\begin{pmatrix} (P_R)\;[P_R] \\ (P_L)\;[P_L] \\ (\hat{T})\;[\hat{T}] \\ (\gamma_5\,\hat{T})\;[\hat{T}] \\ (P_R)\;[P_L] \\ (P_R\gamma^\mu)\;[P_L\gamma_\mu] \\ (P_L)\;[P_R] \\ (P_L\gamma^\mu)\;[P_R\gamma_\mu] \\ (P_R\gamma^\mu)\;[P_R\gamma_\mu] \\ (P_L\gamma^\mu)\;[P_L\gamma_\mu] \end{pmatrix} = \frac{1}{4}\left(\begin{array}{cccc|cc|cc|c|c} 2 & 0 & 1 & 1 & & & & & & \\ 0 & 2 & 1 & -1 & & & & & & \\ 6 & 6 & -2 & 0 & & & & & & \\ 6 & -6 & 0 & 2 & & & & & & \\ \hline & & & & 0 & 2 & & & & \\ & & & & 8 & 0 & & & & \\ \hline & & & & & & 0 & 2 & & \\ & & & & & & 8 & 0 & & \\ \hline & & & & & & & & -4 & 0 \\ \hline & & & & & & & & 0 & -4 \end{array}\right) \begin{pmatrix} (P_R]\;[P_R) \\ (P_L]\;[P_L) \\ (\hat{T}]\;[\hat{T}) \\ (\gamma_5\,\hat{T}]\;[\hat{T}) \\ (P_R]\;[P_L) \\ (P_R\gamma^\mu]\;[P_L\gamma_\mu) \\ (P_L]\;[P_R) \\ (P_L\gamma^\mu]\;[P_R\gamma_\mu) \\ (P_R\gamma^\mu]\;[P_R\gamma_\mu) \\ (P_L\gamma^\mu]\;[P_L\gamma_\mu) \end{pmatrix}. \tag{3}$$

Non-explicit matrix elements in (3) are zero, and we have introduced a shorthand $\hat{T}$ for either $\hat{\Gamma}^T = \frac{1}{2}\sigma^{\mu\nu}$ or $\hat{\Gamma}_T = \frac{1}{2}\sigma_{\mu\nu}$.

The importance of this transformation for us is that it converts t-channel and u-channel exchange graphs into s-channel form, for which it is straightforward to evaluate the partial waves. The block-diagonal structures, delineated with horizontal and vertical lines, show that "mixing" occurs only within the subsets $\{P_R\otimes P_R,\ P_L\otimes P_L,\ \hat{T}\otimes\hat{T},\ \gamma_5\,\hat{T}\otimes\hat{T}\}$, and $\{P_R\otimes P_L,\ P_R\gamma^\mu\otimes P_L\gamma_\mu\}$. The Fierz transform matrix is idempotent, meaning its square is equal to the identity matrix. This follows from the fact that two Fierz rearrangements return the process to its initial ordering. A consequence of the block-diagonal form is that each sub-block is itself idempotent.

In Eq. (3) we have included one non-member of the basis set, namely $\gamma_5\,\hat{T}$; it is connected to $\hat{T}$ via the relation

$$\gamma_5\,\sigma^{\mu\nu} = \frac{i}{2}\epsilon^{\mu\nu\alpha\beta}\sigma_{\alpha\beta}\,. \tag{4}$$

Explicit use of $\gamma_5\,\hat{T}$ in Eq. (3) is an efficient way to express the chiral Fierz transformation.

So far we have not used the qualifier in the assumption, that the dark matter is Majorana. Majorana particles are invariants under charge conjugation C, which implies that vector and tensor bilinears are disallowed. Another way of understanding this is to note that interchanging the two identical Majorana particles in a t-channel diagram generates an accompanying u-channel diagram with a relative minus sign (from fermion anticommutation). When Fierzed, these two amplitudes cancel for V and T couplings (exactly so in the Four-Fermi limit where the differing momenta in the t- and u-channel propagators can be ignored – refer to Appendix B for details). We must thus drop V and T couplings appearing in the Fierzed bilinears of the χ-current.

B. Origin of v^2 and Helicity Suppressions

One can use partial wave decomposition (see. e.g., the textbooks [27–29], or the convenient summary in the Appendix of [8]) to expand the scattering amplitudes as a sum of angular momentum components. Partial waves do not interfere, and the L^{th} partial wave contribution to the total cross section σv is proportional to v^{2L}. The annihilating χ particles are very non-relativistic today, so an unsuppressed s-wave ($L=0$), if present, will dominate the annihilation cross section. The DM virial velocity within our Galaxy is about 10^{-3} (in units of c), leading to a suppression of $v^2 \sim 10^{-6}$ for p-wave processes.

On the other hand, the SM fermions produced in the $2\to 2$ annihilation are highly relativistic (except possibly for $t\bar{t}$ production). For many annihilation channels the spin state of the fermion pair gives rise to a helicity suppression by a factor of $(m_l/M_\chi)^2$, where m_l is the fermion mass.

Unfortunately, many popular models for annihilation of Majorana dark matter to charged leptons are subject to one or more of these two suppressions, the v^2 and/or $(m_\ell/M_\chi)^2$ suppressions. This includes some of the models proposed to accommodate the positron and e^+e^- excesses observed in PAMELA, Fermi-LAT, and HESS data. In Section III, we show that in the class of models which have suppressed rates for $\chi\chi \to \ell^+\ell^-$, the $2 \to 3$ graph obtained by adding a radiative $W^\pm$ or Z to the final state particles of the $2 \to 2$ graph becomes dominant. The radiated W's and Z's will decay to, among other particles, antiprotons. Since an excess generation of antiprotons is not observed by PAMELA, this class of models is ruled out by the present work.

Consider products of s-channel bilinears of the form $(\overline{\chi}\,\Gamma_1\chi)(\bar{l}\,\Gamma_2 l)$. To further address the question of which products of currents are suppressed and which are not, we may set v^2 to zero in the χ-current, and m_ℓ^2 to zero in the lepton current, and ask whether the product of currents is suppressed. If the product of currents is non-zero in this limit, the corresponding amplitude is unsuppressed. In Table I we give the results for the product of all standard Dirac bilinears. (The derivation of these results is outlined in Appendix C.) Suppressed bilinears enter this table as zeroes. [1]

One can read across rows of this table to discover that the only unsuppressed s-channel products of bilinears for the $2 \to 2$ process are those of the pseudo-scalar, vector, and tensor. (For completeness, we also show results for the pseudo-tensor bilinears, although the pseudo-tensor is not independent of the tensor, as a result of Eq. 4.) For Majorana dark matter, the vector and tensor bilinears are disallowed by charge-conjugation arguments and one is left with just the unsuppressed pseudo-scalar.

C. Class of Models for which $\chi\chi \to \ell\bar{\ell}$ Annihilation is Suppressed

We now put the results of the previous two subsections together to explain which class of models have a v^2 and/or $(m_\ell/M_\chi)^2$ suppressed $2 \to 2$ annihilation. We have seen that, for Majorana DM, s-channel annihilation with a P coupling is unsuppressed, while S and A contributions are suppressed (and V and T forbidden). Let us now consider t-channel or u-channel processes.

Any t-channel or u-channel diagram that Fierz's to an s-channel form containing a pseudoscalar coupling will have an unsuppressed $L = 0$ s-wave amplitude. From the matrix in Eq. (3), one deduces that such will be the case for any t- or u-channel current product on the left side which finds a contribution in the 1^{st}, 2^{nd}, 5^{th}, or 7^{th} columns of the right side. This constitutes the t- or u-channel tensor, same-chirality scalar, and opposite chirality vector products (rows 1 through 4, and 6 and 8 on the left). On the other hand, the t- or u-channel opposite chirality scalars or same-chirality vectors (rows 5, 7, 9, and 10 on the left) do *not* contain a pseudoscalar coupling after Fierzing to s-channel form. Rather, it is the suppressed axial-vector and vector (Dirac fermions only) that appears.

Interestingly, a class of the most popular models for fermionic dark matter annihilation to charged leptons, fall into this latter, suppressed, category. It is precisely the opposite-chirality t- or u-channel scalar exchange that appears in these models, an explicit example of which will be discussed below. Thus it is rows 5 and 7 in Eq. (3) that categorize the model we will analyze. After Fierzing to s-channel form, it is seen that the Dirac bilinears are opposite-chirality vectors (i.e., V or A). Dropping the vector term from the χ-current we see that the $2 \to 2$ process couples an axial vector χ-current to a relativistic SM fermion-current which is an equal mixture of A and V. Accordingly, this model has an s-wave amplitude occurring only in the $L = 0$, $J = 1$, $S = 1$ channel, with the spin flip from $S = 0$ to $S = 1$ (or equivalently, the mismatch between zero net chirality and one unit of helicity) costing a fermion mass-insertion and a $(m_f/M_\chi)^2$ suppression in the rate.

Let us pause to explain why this t- or u-channel scalar exchange with opposite fermion chiralities at the vertices is so common. It follows from a single popular assumption, namely that the dark matter is a gauge-singlet Majorana fermion. As a consequence of this assumption, annihilation to SM fermions, which are $SU(2)$ doublets or singlets, requires either an s-channel singlet boson or a t- or u-channel singlet or doublet scalar that couples to χ-f. In the first instance, there is no symmetry to forbid a new force between SM fermions, a disfavored possibility. In the second instance, unitarity fixes the second vertex as the hermitian adjoint of the first. Since the fermions of the SM are left-chiral doublets and right-chiral singlets, one gets chiral-opposites for the two vertices of the t- or u-channel.

Supersymmetry provides an analog of such a model. In this case the dark matter consists of Majorana neutralinos, which annihilate to SM fermions via the exchange of ("right"- and "left"-handed) $SU(2)$-doublet slepton fields. In fact, the implementation in 1983 of supersymmetric photinos as dark matter provided the first explicit calculation of s-wave suppressed Majorana dark matter [30]. However, the class of models described above is more general than the class of supersymmetric models.

To illustrate our arguments, we choose a simple example of the class of model under discussion. This is provided by the leptophilic model proposed in Ref. [31] by Cao, Ma and Shaughnessy. Here the DM consists of a gauge-singlet Majorana fermion χ which annihilates to

[1] It is seen that the only bilinears in the table without velocity-suppression are those of the pseudo-scalar, the three-vector part of the vector, the zero$^{\rm th}$ component of the axial vector, and the time-space part of the tensor (or equivalently, the space-space part of the pseudotensor). It is also seen that the only bilinears without fermion mass-suppression are the scalar, pseudoscalar, three-vector parts of the vector and axial vector, and the tensor.

s-channel bilinear $\bar{\Psi}\,\Gamma_D\,\Psi$		$v=0$ limit		$M=0$ limit	
		parallel spinors	antiparallel spinors	parallel spinors	antiparallel spinors
scalar	$\bar{\Psi}\,\Psi$	0	0	$\sqrt{s}$	0
pseudo-scalar	$\bar{\Psi}\,i\gamma_5\,\Psi$	$-2iM$	0	$-i\sqrt{s}$	0
axial-vector	$\bar{\Psi}\,\gamma_5\,\gamma^0\,\Psi$	$2M$	0	0	0
	$\bar{\Psi}\,\gamma_5\,\gamma^j\,\Psi$	0	0	0	$\sqrt{s}\,(\pm\delta_{j1}-i\delta_{j2})$
vector	$\bar{\Psi}\,\gamma^0\,\Psi$	0	0	0	0
	$\bar{\Psi}\,\gamma^j\,\Psi$	$\mp 2M\,\delta_{j3}$	$-2M\,(\delta_{j1}\mp i\delta_{j2})$	0	$-\sqrt{s}\,(\delta_{j1}\mp i\delta_{j2})$
tensor	$\bar{\Psi}\,\sigma^{0j}\,\Psi$	$\mp 2iM\,\delta_{j3}$	$-2iM\,(\delta_{j1}\pm\delta_{j2})$	$-i\sqrt{s}\,\delta_{j3}$	0
	$\bar{\Psi}\,\sigma^{jk}\,\Psi$	0	0	$\pm\sqrt{s}\,\delta_{j1}\delta_{k2}$	0
pseudo-tensor	$\bar{\Psi}\,\gamma_5\,\sigma^{0j}\,\Psi$	0	0	$\pm i\sqrt{s}\,\delta_{j3}$	0
	$\bar{\Psi}\,\gamma_5\,\sigma^{jk}\,\Psi$	$\mp 2M\,\delta_{j1}\delta_{k2}$	$-2M\,(\delta_{j2}\delta_{k3}\mp i\delta_{j3}\delta_{k1})$	$-\sqrt{s}\,\delta_{j1}\delta_{k2}$	0

TABLE I. Extreme non-relativistic and extreme relativistic limits for s-channel bilinears. In order for a term with an initial-state DM bilinear and a final-state lepton bilinear to remain unsuppressed, the DM bilinear must have a non-zero entry in the appropriate cell of the "$v=0$ limit" columns, and the lepton bilinear must have a non-zero term in the appropriate cell of the "$M=0$ limit" columns. Otherwise, the term is suppressed. (The tensor and pseudo-tensor are not independent, but rather are related by $\gamma_5\,\sigma^{\mu\nu}=\frac{i}{2}\epsilon^{\mu\nu\alpha\beta}\,\sigma_{\alpha\beta}$.) We recall that antiparallel spinors correspond to parallel particle spins (and antiparallel particle helicities for the $M=0$ current), and vice versa. Amplitudes are shown for $\overline{u}\,\Gamma_D\,v=[\overline{v}\,\Gamma_D\,u]^*$. The two-fold $\pm$ ambiguities reflect the two-fold spin assignments for parallel spins, and separately for antiparallel spins.

leptons via the $SU(2)$-invariant interaction term

$$f\left(\nu\,\ell^-\right)_L\,\varepsilon\begin{pmatrix}\eta^+\\ \eta^0\end{pmatrix}\chi+h.c.=f(\nu_L\eta^0-\ell_L\eta^+)\chi+h.c. \tag{5}$$

where f is a coupling constant, ε is the 2×2 antisymmetric matrix, and $(\eta^+,\,\eta^0)$ form the new $SU(2)$ doublet scalar which mediates the annihilation. (This model was originally discussed in Ref. [32], and an expanded discussion of its cosmology may be found in Ref. [33].)

As discussed above, the u- and t-channel amplitudes for DM annihilation to leptons, of the form $(\overline{\chi}P_L l)\,(\bar{l}P_R\chi)$, become pure $(\overline{\chi}P_L\gamma^\mu\chi)\,(\bar{l}P_R\gamma_\mu l)$ under the chiral Fierz transformation. The product of the Majorana and fermion bilinears then leads to an AA term and an AV term. However, reference to Table I shows that neither of these terms leads to an unsuppressed amplitude: in all cases, either the lepton bilinear is suppressed by m_ℓ, the DM bilinear by v, or both are suppressed. Thus, Majorana DM annihilation to a lepton pair is suppressed in this model, in accordance with the explicit calculation in Ref. [31].

III. LIFTING THE SUPPRESSION

Allowing the lepton bilinear to radiate a W or Z boson (as shown in Fig. (1)) does yield an unsuppressed amplitude. In the rate, there will be the usual radiative suppression factor of $\frac{\alpha_2}{4\pi}\sim 10^{-3}$. But, this will be partially compensated by a 3-body phase space factor $\sim(M_\chi/M_W)^2/8\pi^2$ relative to 2-body massless phase space, which exceeds unity for dark matter masses exceeding $\sim$TeV. (When $M_\chi^2\gg M_W^2$, the rate for radiative production of W's is so large that resummation techniques become necessary. The result is the well-known $\ln^2(M_\chi/M_W)$ taming of the production rate [34].) More importantly, the v^2 suppression for Majorana annihilation to 2-body final states will be lifted by the 3-body W-bremsstrahlung process. In Section IV we show, by explicit calculation, that the $2\to 3$ radiative process that leads to antiprotons dominates for any M_χ that allows the W to be produced on-shell, i.e., for $2M_\chi>M_W$.

The next inevitable question is "Why is the radiative $2\to 3$ process unsuppressed?" To answer this question, we invoke a more general Fierz rearrangement applicable to $2\to N$ processes, $N\geq 3$. The relevant equation, derived in Appendix A states that any 4×4 matrices X and Y may be expressed as

$$\begin{aligned}(\mathrm{X})\,[\mathrm{Y}]&=(\mathrm{X}\mathbb{1})\;[\mathbb{1}\mathrm{Y}]\\ &=\frac{1}{4}\,(\mathrm{X}\,\Gamma^B\,\mathrm{Y}\,]\;[\,\Gamma_B\,)\\ &=\frac{1}{4^2}\,Tr\,[\mathrm{X}\,\Gamma^B\,\mathrm{Y}\,\Gamma_C]\;(\Gamma^C\,]\;[\Gamma_B\,)\,,\end{aligned} \tag{6}$$

where the Dirac matrices here are taken in the standard basis defined in Eq. (A1).

From Table (I) we see that setting Γ^C to $\gamma_5\,\gamma^0$, the only structure available to a non-relativistic Majorana current other than the pseudoscalar, and Γ_B to either γ^j or $\gamma_5\gamma^j$, provides an unsuppressed product of the Majorana dark matter bilinear and the charged lepton bilinear. Moreover, for the W/Z-bremsstrahlung process, X and Y in the general Fierz equation are the un-Fierzed couplings P_L and $q^{-2}\,P_R\,\not{q}\,P_L\,\not{\epsilon}$, respectively. So we will have shown that the radiative process is unsuppressed if we

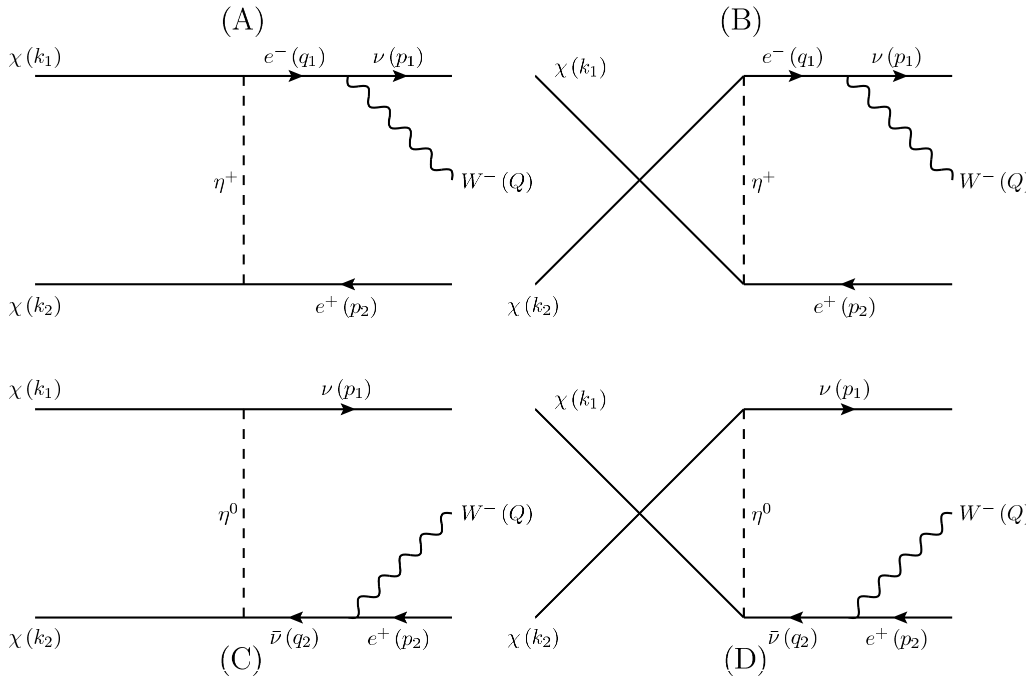

FIG. 1. t-channel (A and C) and u-channel (B and D) contributions to $\chi\chi \to e^+\nu W^-$. Emission from the scalar propagator is not included, as it is suppressed by $1/M_\eta^2$. Note that all fermion momenta flow with the arrow except p_2, so $q_1 = p_1 + Q$, $q_2 = -p_2 - Q$.

can show that $q^{-2}\,Tr\,[P_L\,(\gamma^j \text{ or } \gamma_5\gamma^j)\,P_R\,\not{q}\,P_L\,\not{\epsilon}\,\gamma_5\,\gamma_0]$ is unsuppressed. This trace reduces to $q^{-2}\,Tr\,[P_R\,\gamma_0\,\gamma^j\,\not{q}\,\not{\epsilon}]$. The expansion of this trace as scalar products contains terms such as $q_0\cdot\epsilon^j$ and $(\vec{\epsilon}\times\vec{q})^j$, which are nonzero and unsuppressed by fermion masses. Thus, the $2\to 3$ process contains an unsuppressed s-wave amplitude.

Physically, the un-suppression works because the gauge boson carries away a unit of angular momentum, allowing a fermion spin-flip such that there is no longer a mismatch between the chirality of the leptons and their allowed two-particle spin state.

One may ask why emission of a gamma-ray rather than a W/Z boson is less effectual. It has been known for some time [4, 5] that gamma-ray emission in the final state does produce an unsuppressed s-wave contribution, but at second order rather than lowest order in the inverse mass-squared M_η^{-2} of the t- and u-channel exchange particle(s). The reason is that gamma-ray emission from the final state fermions (FSR) is dominated by infra-red and collinear singularities, each of which puts the intermediate lepton on-shell (virtuality $q^2\to 0$). Including the q^{-4} from the squared propagator in the phase space integral (see Eq. (20)), one gets the factor $\int_{M_V^2}^{s}\frac{dq^2}{q^6}(s-q^2)\,(q^2-M_V^2)$, where M_V is the mass of the radiated boson (photon or W or Z). For a gamma-ray, with $M_V^2=0$, one readily sees the infra-red and collinear singularities in $\int_0\frac{dq^2}{q^4}$. An on-shell particle is observable, so the spin states of the $q^2\to 0$ intermediate fermion do not interfere. Thus, as $q^2\to 0$, the trace for gamma emission, $Tr\,[\gamma_0\,\gamma^j\,\not{q}\,\not{\epsilon}] = Tr\,[\gamma_0\,\gamma^j\,(P_R^2+P_L^2)\not{q}\,\not{\epsilon}]$ goes over to $Tr\,[\gamma_0\,\gamma^j\,P_R]\,[P_R\not{q}\,\not{\epsilon}] + Tr\,[\gamma_0\,\gamma^j\,P_L]\,[P_L\not{q}\,\not{\epsilon}]$. The first trace in each term of this sum vanishes. Consequently, the gamma-emission amplitude remains suppressed at order M_η^{-2}. However, at order M_η^{-4}, the gamma-ray may be emitted from the internal particle η (VIB). For VIB, phase space does not favor $q^2=0$, and an unsuppressed amplitude results.

The emission of a massive W (or Z) boson contrasts significantly from the emission of a massless photon. With the W emission, the relevant phase space integral over virtuality q^2 is $\int_{M_W^2}^{s}\frac{dq^2}{q^6}(s-q^2)\,(q^2-M_W^2)$. The minimum virtuality of the intermediate fermion is $q^2=M_W^2$, and the mean virtuality for $s\gg M_W^2$ is greater again by the factor $2\ln(s/M_W^2)$. With no infra-red or collinear singularities for W/Z-emission, an unsuppressed amplitude results already at order M_η^{-2}.

Before looking at an explicit example in which electroweak bremsstrahlung is seen to lift a suppression, we pause to summarize some important facts for the $2\to 2$ annihilation process:

- Fierz transformation is used to re-express t- and u-channel amplitudes of the form $(\overline{\chi}\,\hat{\Gamma}^A l)(\bar{l}\,\hat{\Gamma}_B\chi)$ as a sum of s-channel (not to be confused with s-wave) amplitudes of the form $(\overline{\chi}\,\hat{\Gamma}^C\chi)(\bar{l}\,\hat{\Gamma}_D l)$.

- For Majorana dark matter, only S, P, and A s-channel bilinears are allowed, with the V and T

bilinears forbidden by the self-conjugate properties of Majorana particles.

- Considering the product of an s-channel χ-current with an s-channel fermion-current, we find that the pseudo-scalar is the only member of the set (S, P, A) which is unsuppressed. The other combinations are either helicity (m_ℓ/m_χ) or velocity (v) suppressed.

- The annihilation process $\chi\chi \to \ell\bar{\ell}$ via t- and u-channel exchange of a scalar is suppressed. Importantly, electroweak bremsstrahlung lifts this suppression at lowest order in the propagator mass-squared (M_η^{-2} in amplitude), whereas photon bremsstrahlung lifts the suppression at the next order (M_η^{-4} in amplitude).

Amplification of the latter remark is the purpose of this paper.

IV. EXPLICIT CALCULATION OF SUPPRESSION-LIFTING WITH ELECTROWEAK BREMSSTRAHLUNG

To explicitly demonstrate that emission of a $W^\pm$ or Z boson does lift helicity suppression, we calculate the cross section for $\chi\chi \to \mathrm{e}^\mp \overset{(-)}{\nu} W^\pm$ below in the leptophilic model of Ref [31]. The interaction term for this model is that given above in Eq. (5).

A. Example of Helicity-Suppressed Rate: Ma's Model

In the model of ref. [31], the cross section for the $2 \to 2$ process $\chi\chi \to \mathrm{e}^+e^-$ or $\nu\bar{\nu}$ with Majorana DM is given as

$$v\,\sigma = \frac{f^4 v^2 r^2}{24\pi\, M_\chi^2}\left(1 - 2r + 2r^2\right), \tag{7}$$

where $m_l \simeq 0$ and $M_{\eta^\pm} = M_{\eta^0}$ have been assumed, and $r = M_\chi^2/(M_\eta^2 + M_\chi^2)$. The suppressions discussed in Section II are apparent in Eq. (7). The helicity suppressed s-wave term is absent in the $m_l = 0$ limit, and thus only the v^2-suppressed term remains.

This $2 \to 2$ cross-section can be calculated by inclusion of two Feynman diagrams, a t-channel exchange of η and the associated u-channel exchange obtained by crossing the Majorana particles. The relative sign between the graphs is negative, due to the fermion exchange. Summing and squaring, one has three terms including the interference term. Alternatively, one may Fierz transform the fermion bilinears in the two contributing amplitudes. The relative minus sign is compensated by the special Majorana minus sign described in Eq. (B2). Reference to Eq. (3) then shows that one gets $(P_L)\,[P_R] \to \frac{1}{2}\,(P_L\gamma^\mu]\,[P_R\gamma_\mu)\times 2$, where the final factor of 2 counts the two contributing amplitudes, which are identical in the four-fermi limit $M_\eta^2 \gg t$ and u. We are left with just one amplitude, $\frac{f^2}{M_\eta^2}[\overline{v}(k_2)(\frac{1}{2}\gamma_5)v(p_2)]\,[\overline{u}(p_1)P_L\gamma_\mu v(p_2)]$. The surviving Dirac structure for the Majorana current is pure axial vector, since the vector (and tensor) part of a Majorana current vanishes. With just a single product of bilinears, the remaining part of the $2 \to 2$ calculation is straightforward. One arrives at

$$v\,\sigma = \frac{f^4\, M_\chi^2}{16\pi\, M_\eta^4}\left[\frac{m_l^2}{s} + \frac{2}{3}v^2 + \mathcal{O}(v^4)\right], \tag{8}$$

in agreement with the four-fermi, $m_\ell = 0$ limit of Eq. (7). Here, the helicity suppression of the s-wave amplitude, proportional to a helicity flip, in turn proportional to a mass insertion, is manifest.

B. W Emission and Unsuppressed S-wave

We now turn to the calculation of the cross section for the process $\chi\chi \to e^+\nu W^-$ (equal to that for $\chi\chi \to e^-\bar{\nu}W^+$). The four contributing Feynman diagrams are shown in Fig. 1. Note that we consider bremsstrahlung only from the final state particles[2] (FSR), and neglect emission from the virtual scalar (VIB). Strictly speaking, the distinction between FSR and VIB is somewhat artificial in the sense that the partition depends upon the choice of gauge. However, we shall work in unitary gauge, in which emission from the internal line is suppressed by a further power of M_η^2 due to the additional scalar propagator; consequently, we expect our results to be valid to order M_η^{-2} in amplitude, i.e. order M_η^{-4} in rate.

We retain the assumptions $m_l \simeq 0$ and $M_{\eta^\pm} = M_{\eta^0}$. The matrix element for the top-left diagram is

$$\mathcal{M}_A = \frac{igf^2}{\sqrt{2}q_1^2}\frac{1}{t_1 - M_\eta^2}\Big(\bar{v}(k_2)P_L v(p_2)\Big) \times\Big(\bar{u}(p_1)\gamma^\mu P_L \not{q}_1 u(k_1)\Big)\epsilon_\mu^Q. \tag{9}$$

where $i\frac{g}{\sqrt{2}}\gamma^\mu P_L$ is the coupling at the $\ell\nu W$ vertex, and

[2] In [10] it was pointed out that subtle gauge cancellations between radiation from the *initial state* particles and the *final state* particles can remove the leading order terms, leaving a greatly suppressed net rate. The example calculation [10] assumed a new $U(1)$ gauge particle that connects the initial dark matter to the final Standard Model states. The lessons learned do not apply to our calculation, since we assume the dark matter is a singlet under the relevant electroweak gauge group (so there is no initial state radiation of W/Z's), and since the sector connectors are new scalar bosons rather than new gauge bosons. Similar remarks decouple the lessons learned from our earlier work [8], contrary to remarks made in [10].

t_1, t_2, u_1, u_2 are the standard Mandelstam variables,

$$\begin{aligned} t_1 &= (k_1 - q_1)^2 = (p_2 - k_2)^2 \\ t_2 &= (k_1 - p_1)^2 = (-q_2 - k_2)^2 \\ u_1 &= (k_2 - q_1)^2 = (p_2 - k_1)^2 \\ u_2 &= (k_2 - p_1)^2 = (-q_2 - k_1)^2. \end{aligned} \tag{10}$$

Upon applying Eq (3) to Fierz transform the matrix element, we obtain

$$\begin{aligned} \mathcal{M}_A = & \frac{igf^2}{\sqrt{2}q_1^2}\frac{1}{t_1 - M_\eta^2}\epsilon_\mu^Q \frac{1}{4} \\ & \Big[\Big(\bar{v}(k_2)u(k_1)\Big)\Big(\bar{u}(p_1)P_L\gamma^\mu P_L \not{q}_1 v(p_2)\Big) \\ & +\Big(\bar{v}(k_2)\gamma_5 u(k_1)\Big)\Big(\bar{u}(p_1)P_L\gamma_5\gamma^\mu P_L \not{q}_1 v(p_2)\Big) \\ & +\Big(\bar{v}(k_2)\gamma_5\gamma_\alpha u(k_1)\Big)\Big(\bar{u}(p_1)\gamma^\alpha\gamma^\mu P_L \not{q}_1 v(p_2)\Big)\Big] \\ = & \frac{igf^2}{\sqrt{2}q_1^2}\frac{1}{t_1 - M_\eta^2}\epsilon_\mu^Q \frac{1}{4} \\ & \times \Big(\bar{v}(k_2)\gamma_5\gamma_\alpha u(k_1)\Big)\Big(\bar{u}(p_1)P_L\gamma^\alpha\gamma^\mu \not{q}_1 v(p_2)\Big). \end{aligned} \tag{11}$$

The first two terms after the first equality are zero due to the helicity projection operators, leaving only an axial vector term. (Vector and tensor χ-bilinears have been omitted, as they will cancel between u and t channel diagrams in the heavy M_η limit, as discussed above.) Note that although this matrix element resembles that of an s-channel annihilation process, the γ matrices in the lepton bilinear would be in a different order for a true s-channel annihilation process involving W/Z-bremsstrahlung from one of the final state leptons.

Similarly, the matrix element for the top-right diagram can be written as

$$\begin{aligned} \mathcal{M}_B = & \frac{-igf^2}{\sqrt{2}q_1^2}\frac{1}{u_1 - M_\eta^2}\frac{1}{4}\Big(\bar{v}(k_2)\gamma_5\gamma_\alpha u(k_1)\Big) \\ & \times\Big(\bar{u}(p_1)P_L\gamma^\alpha\gamma^\mu \not{q}_1 v(p_2)\Big)\epsilon_\mu^Q, \end{aligned} \tag{12}$$

and those for the bottom diagrams,

$$\begin{aligned} \mathcal{M}_C = & \frac{-igf^2}{\sqrt{2}q_2^2}\frac{1}{t_2 - M_\eta^2}\frac{1}{4}\Big(\bar{v}(k_2)\gamma_5\gamma_\alpha u(k_1)\Big) \\ & \times\Big(\bar{u}(p_1)P_L \not{q}_2\gamma^\mu\gamma^\alpha v(p_2)\Big)\epsilon_\mu^Q, \end{aligned} \tag{13}$$

$$\begin{aligned} \mathcal{M}_D = & \frac{igf^2}{\sqrt{2}q_2^2}\frac{1}{u_2 - M_\eta^2}\frac{1}{4}\Big(\bar{v}(k_2)\gamma_5\gamma_\alpha u(k_1)\Big) \\ & \times\Big(\bar{u}(p_1)P_L \not{q}_2\gamma^\mu\gamma^\alpha v(p_2)\Big)\epsilon_\mu^Q. \end{aligned} \tag{14}$$

Performing the sum over spins and polarizations, we find

$$\begin{aligned} & \sum_{\text{spin, pol.}} |\mathcal{M}|^2 = \sum_{\text{spin, pol.}} |\,(\mathcal{M}_A + \mathcal{M}_C) - (\mathcal{M}_B + \mathcal{M}_D)\,|^2 \\ = & \left(\frac{gf^2}{\sqrt{2}}\right)^2 \frac{1}{16}\mathrm{Tr}\left[(\not{k}_2 + M_\chi)\gamma_\alpha(\not{k}_1 + M_\chi)\gamma_\beta\right]\left(g_{\mu\nu} - \frac{Q_\mu Q_\nu}{M_W^2}\right)\left(\frac{1}{q_1^4}\left(\frac{1}{t_1 - M_\eta^2} + \frac{1}{u_1 - M_\eta^2}\right)^2 \mathrm{Tr}\Big[\not{p}_1\gamma^\alpha\gamma^\mu\not{q}_1\,\not{p}_2\,\not{q}_1\,\gamma^\nu\gamma^\beta P_R\Big]\right. \\ & -\frac{1}{q_1^2 q_2^2}\left(\frac{1}{t_1 - M_\eta^2} + \frac{1}{u_1 - M_\eta^2}\right)\left(\frac{1}{t_2 - M_\eta^2} + \frac{1}{u_2 - M_\eta^2}\right)\left(\mathrm{Tr}\Big[\not{p}_1\gamma^\alpha\gamma^\mu\not{q}_1\,\not{p}_2\,\gamma^\beta\gamma^\nu\not{q}_2\,P_R\Big] + \mathrm{Tr}\Big[\not{p}_1\not{q}_2\gamma^\mu\gamma^\alpha\,\not{p}_2\,\not{q}_1\,\gamma^\nu\gamma^\beta P_R\Big]\right) \\ & \left.+\frac{1}{q_2^4}\left(\frac{1}{t_2 - M_\eta^2} + \frac{1}{u_2 - M_\eta^2}\right)^2 \mathrm{Tr}\Big[\not{p}_1\not{q}_2\gamma^\mu\gamma^\alpha\,\not{p}_2\,\gamma^\beta\gamma^\nu\not{q}_2\,P_R\Big]\right) \end{aligned} \tag{15}$$

We evaluate this in terms of scalar products using the standard Dirac Algebra, leading to a result too lengthy to record here.

The thermally-averaged rate is given by

$$v\,d\sigma = \frac{1}{2s}\int \frac{1}{4}\sum_{\text{spin, pol.}} |\mathcal{M}|^2\, dLips^3 \tag{16}$$

where the $\frac{1}{4}$ arises from averaging over the spins of the initial χ pair, and $v = \sqrt{1 - \frac{4M_\chi^2}{s}}$ is the mean dark matter relative velocity, as well as the dark matter single-particle velocity in the center of mass frame[3].

The three-body Lorentz Invariant Phase Space is

$$dLips^3 = (2\pi)^4 \frac{d^3\vec{p}_1}{2E_1}\frac{d^3\vec{p}_2}{2E_2}\frac{d^3\vec{Q}}{2E_W}\frac{\delta^4(P - p_1 - p_2 - Q)}{(2\pi)^9} \tag{17}$$

and $P = k_1 + k_2$. This factorizes into the product of two two-body phase space integrals, convolved with an

[3] Informative discussions of the meaning of v are given in [35], and, including thermal averaging, in [36].

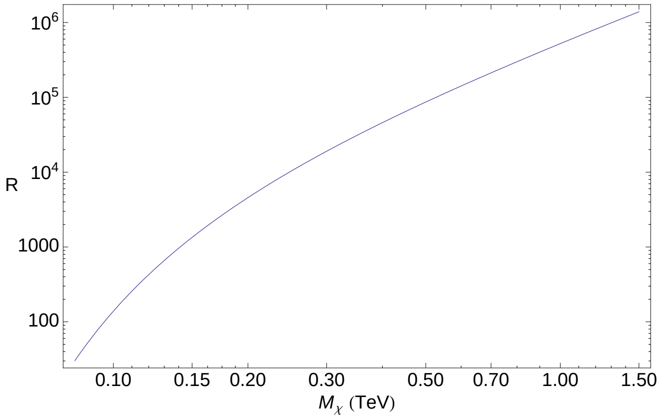

FIG. 2. The ratio $R = v\,\sigma(\chi\chi \to e^+\nu W^-)/v\,\sigma(\chi\chi \to e^+e^-)$ for the example model [31], with $M_\eta^2 \gg M_\chi^2$. We have used $v = 10^{-3}c$, appropriate for the Galactic halo.

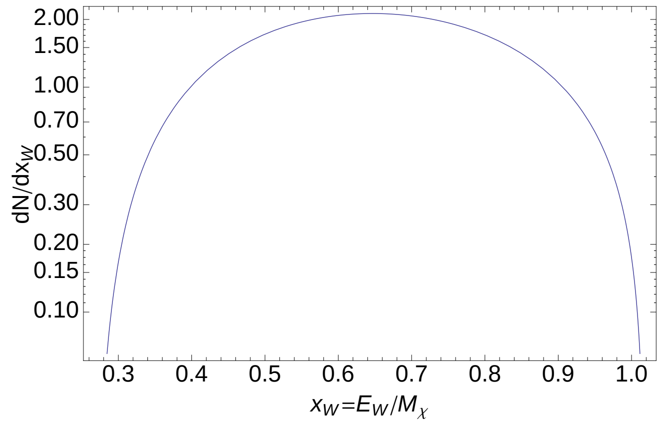

FIG. 3. The W spectrum per $\chi\chi \to e\nu W$ event for the example model, with $M_\chi = 300$ GeV and $M_\eta^2 \gg M_\chi^2$.

integral over the fermion propagator momentum,

$$dLips^3 = \int_{M_W^2}^s \frac{dq_1^2}{2\pi}\left(\frac{d^3\vec{q}_1}{2E_{q_1}}\frac{d^3\vec{p}_2}{2E_2}\frac{\delta^4(P-q_1-p_2)}{(2\pi)^2}\right) \times \left(\frac{d^3\vec{p}_1}{2E_1}\frac{d^3\vec{Q}}{2E_W}\frac{\delta^4(q_1-Q-p_1)}{(2\pi)^2}\right) = \int_{M_W^2}^s \frac{dq_1^2}{2\pi}\, dLips^2(P^2,q_1^2,p_2^2)\, dLips^2(q_1^2,Q^2,p_1^2). \quad (18)$$

Evaluating the two-body phase space factors in their respective center of momentum frames, and using $p_1^2 = p_2^2 = 0$, we have

$$dLips^2(x^2,y^2,0) = \frac{x^2-y^2}{8\pi x^2}\frac{d\bar{\Omega}}{4\pi}. \quad (19)$$

This allow us to write the three-body phase space as

$$dLips^3 = \frac{1}{2^6(2\pi)^4}\int_{M_W^2}^s dq_1^2 \times \frac{(s-q_1^2)(q_1^2-Q^2)}{sq_1^2}\, d\phi\, d\cos\theta_P\, d\cos\theta_q, \quad (20)$$

where ϕ is the angle of intersection of the plane defined by $\chi\chi \to ee^*$ with that defined by $e\nu W$, and θ_P and θ_q are defined in P (CoM) and q rest frames respectively.

We evaluate the scalar products that arise from Eq.(15) in terms of the invariants q_1^2, $Q^2 = M_W^2$, s, t_1, and u_1, and the angles θ_P, θ_q, and ϕ. We then use Eq. (16) to evaluate the cross section. As we have neglected diagrams suppressed by M_η^{-2} relative to those in Fig. 1, we present our results to leading order in M_η^{-4} (i.e., we take $M_\eta^2 \gg t_1, t_2, u_1, u_2$). To leading order in powers of M_χ and M_W in the numerator, we find

$$v\,\sigma = \frac{g^2 f^4}{512 M_W^2 M_\eta^4 \pi^3}\Bigg\{ M_\chi^4\left(\frac{1}{3}\ln\left[\frac{4M_\chi^2}{M_W^2}\right] - \frac{7}{18}\right) + M_\chi^2 M_W^2 \Bigg(\ln\left[\frac{4M_\chi^2}{M_W^2}\right]\left\{1+\ln\left[\frac{2M_W M_\chi}{M_W^2+4M_\chi^2}\right]\right\} - 1 + \mathrm{Li}_2\left[\frac{4M_\chi^2}{M_W^2+4M_\chi^2}\right] - \mathrm{Li}_2\left[\frac{M_W^2}{M_W^2+4M_\chi^2}\right]\Bigg) + \mathcal{O}(M_W^4)\Bigg\}. \quad (21)$$

The Spence function (or "dilogarithm") is defined as $\mathrm{Li}_2(z) \equiv -\int_0^z \frac{d\zeta}{\zeta}\ln|1-\zeta| = \sum_{k=1}^\infty \frac{z^k}{k^2}$. The full expression (retaining sub-leading terms in M_χ in the numerator) is specified in Appendix D. Clearly, the leading terms are neither helicity nor velocity suppressed.

The effectiveness of the W-strahlung processes in lifting suppression of the annihilation rate can be seen Fig. 2, where we plot the ratio of the W-strahlung cross section to that of the lowest order process, $R_W = v\,\sigma(\chi\chi \to e^+\nu W^-)/v\,\sigma(\chi\chi \to e^+e^-)$. We see that W-strahlung dominates over the lowest order annihilation process, for all DM masses above the W production threshold. The W-bremsstrahlung rate rises approximately as M_χ^4. As M_χ^2 increases, eventually phase space allows multi-W/Z radiative production, with such a large rate that resummation techniques become necessary, taming the growth with a $\ln^2(M_\chi/M_W)$ factor [34]. The onset of multi-W/Z dominance has been discussed in [6–8].

To obtain the energy spectrum of the W, we compute the differential cross section in terms of E_W by making the transformation

$$d\cos(\theta_q) \to \frac{-4\sqrt{s}q^2}{(s-q^2)(q^2-M_W^2)}dE_W. \quad (22)$$

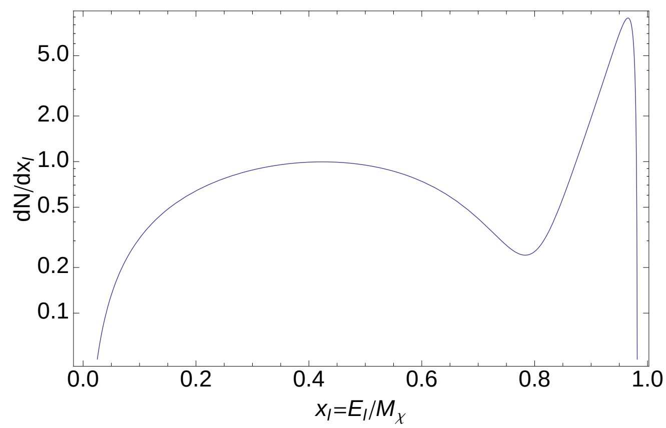

FIG. 4. The primary lepton spectrum per $\chi\chi \to e\nu W$ for the example model, with $M_\chi = 300$ GeV and $M_\eta^2 \gg M_\chi^2$.

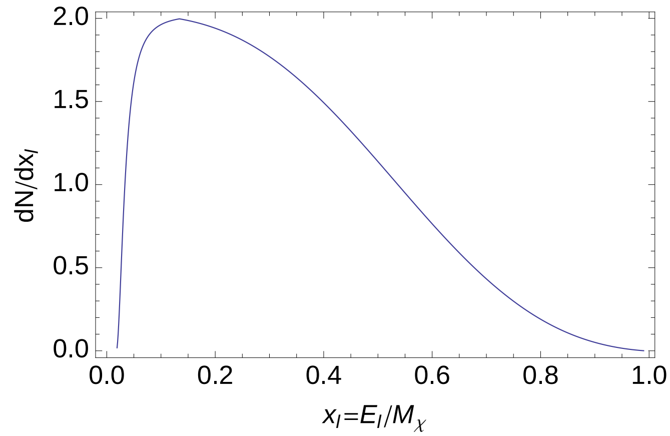

FIG. 5. The secondary lepton spectrum (i.e., from $W \to \nu_\ell \ell$) per W for the example model, with $M_\chi = 300$ GeV and $M_\eta^2 \gg M_\chi^2$. (The branching ratio for $W \to \nu l$, 11% per flavor, is not included here.)

We find [37], again to leading order M_η^{-4},

$$\frac{v\,d\sigma}{dE_W} = \frac{g^2 f^4}{512 E_W M_W^2 M_\eta^4 \pi^3}$$
$$\times \Bigg\{ 2E_W \sqrt{E_W^2 - M_W^2}\left(M_W^2 - 6E_W^2 + 8E_W M_\chi - 2M_\chi^2\right)$$
$$+ \Big(4E_W^4 - 8E_W^3 M_\chi + (2E_W^2 - M_W^2)\left(2M_\chi^2 + M_W^2\right)\Big)$$
$$\times \ln\left[\frac{E_W + \sqrt{E_W^2 - M_W^2}}{E_W - \sqrt{E_W^2 - M_W^2}}\right]\Bigg\}. \tag{23}$$

The W spectrum per $\chi\chi \to e\nu W$ event is given in Fig. 3. We use the scaling variable $x_W \equiv E_W/M_\chi$, and plot $dN/dx_W \equiv (\frac{1}{\sigma_{e^+\nu W^-}})\frac{d\sigma_{e^+\nu W^-}}{dx_W}$. The kinematic range of x_w is $[\frac{M_W}{M_\chi},\ (1+\frac{M_W^2}{4M_\chi^2})]$, with the lower limit corresponding to a W produced at rest, and the upper limit corresponding to parallel lepton momenta balancing the opposite W momentum. As evident in Fig. 3, the W boson spectrum has a broad energy distribution, including a significant component at high energy $E_W \sim M_\chi$.

The energy spectrum of the the primary leptons is calculated in similar fashion. We present the analytic result in Appendix D (along with more detailed expressions for $v\,\sigma$ and $v\,d\sigma/dE_W$). Here the range of the scaling variable $x_\ell \equiv E_\ell/M_\chi$ is $[\,0,\,1-\frac{M_W^2}{4M_\chi^2}]$. Both limits arise when one lepton has zero energy and the other is produced back-to-back with the W. The lepton spectrum is shown in Fig. 4. Note that this lepton spectrum is valid for either e^+ or ν from the annihilation $\chi\chi \to e^+\nu W^-$, and for either e^- or $\bar\nu$ from the annihilation $\chi\chi \to e^-\bar\nu W^+$. The primary lepton spectrum in Fig. 4 features a sharp cut off near $E_\ell = M_\chi$, and a dip in the spectrum that is due to an absorptive interference effect.

To obtain the full lepton spectrum, the contributions from the subsequent decays of the gauge bosons to leptons must be included. (The contribution from the lowest order $2 \to 2$ process $\chi\chi \to e^+e^-$ or $\nu\bar\nu$ is negligible. We also neglect final state leptons resulting from μ decay and from the τ decay chain. These leptons are softer than those we consider.) For leptons from W-decay, the range of the scaling variable x_ℓ is $[\frac{M_W^2}{4M_\chi^2},\,1]$. These limits arise when all four final state lepton momenta are collinear. Particle spectra from the W decay may be calculated in a simple but approximate way, as we describe in Appendix E leading to Eq. (E8). The resulting secondary lepton spectrum is shown in Fig (5). Unsurprisingly, the spectrum of secondary leptons is softer than the spectrum of primary leptons.

When combining the primary lepton and secondary lepton spectra, the relative weights are model dependent. For example, the primary ℓ-spectrum is weighted by $BR(\chi\chi \to W\nu\ell) + 2BR(\chi\chi \to Z\ell\ell)$, while the secondary ℓ-spectrum is weighted by $BR(\chi\chi \to W+X) \times BR(W \to \nu\ell) + BR(\chi\chi \to Z+X) \times BR(Z \to \ell\ell)$.

We note that the final charged-lepton spectra will by modified by cosmic propagation effects. The injected $e^\pm$ will suffer rapid energy losses from synchrotron and inverse Compton processes on the Universe's background magnetic and radiation fields (see, e.g., Ref. [38] for a recent analysis). On the other hand, the injected neutrinos do not interact with the environment, and so their spectra remain unmodified.

C. Unsuppressed Z Emission

Consider the process producing the $\bar\nu\nu Z$ final state. The cross sections for the Z-strahlung processes are related to those for W-strahlung in a simple way: The amplitudes producing $\bar\nu\nu Z$ arise from the same four graphs of Fig. (1), where e, W and η^+ are replaced everywhere by ν and Z and η_0, respectively. The calculation of the amplitudes, and their interferences, thus proceeds in an identical fashion. After making the replacement

$M_W \to M_Z$, the cross section for the annihilation process $\chi\chi \to \nu\bar{\nu}Z$ differs from that for $\chi\chi \to e^+\nu W^-$ by only an overall normalization factor,

$$v\,\sigma_{\nu\bar{\nu}Z} = \frac{1}{(2\cos^2\theta_W)} \times v\,\sigma_{e^+\nu W^-}\Big|_{M_W\to M_Z} \simeq 0.65 \times v\,\sigma_{e^+\nu W^-}\Big|_{M_W\to M_Z}. \quad (24)$$

Consider now the e^+e^-Z final state. Again, the amplitudes arise from the same four basic graphs of Fig. (1). Since only the left-handed leptons couple to the dark matter via the SU(2) doublet η, only the left handed component of e^- participates in the interaction with the Z. Therefore, the couplings of the charged leptons to Z and W take the same form, up to a normalization constant. We thus find

$$v\,\sigma_{e^+e^-Z} = \frac{2\left(\sin^2\theta_W - \frac{1}{2}\right)^2}{\cos^2\theta_W} \times v\,\sigma_{e^+\nu W^-}\Big|_{M_W\to M_Z} \simeq 0.19 \times \; v\,\sigma_{e^+\nu W^-}\Big|_{M_W\to M_Z}. \quad (25)$$

V. CONCLUSIONS

In an attempt to explain recent anomalies in cosmic ray data in a dark matter framework, various non-standard properties have been invoked such as dominant annihilation to leptons in so-called leptophilic models. When the dark matter is Majorana in nature, such annihilations invariably are confronted by suppressions of such processes via either p-wave velocity suppression or helicity suppression. With the aid of Fierz transformation technology, which we have presented in some detail, we have elucidated the general circumstances where suppressions may be encountered.

It has been known for some time that photon bremsstrahlung may have a dramatic effect on such suppressions. We have shown that once one considers the inclusion of three body final states due to electroweak bremsstrahlung, one may also lift these suppressions and obtain rates which may be several orders of magnitude beyond those without such radiative corrections. In fact, barring an unexpected mass-degeneracy, the EW-bremsstrahlung lifts the suppression at one order lower in a certain small ratio of squared masses than does EM-bremsstrahlung, as explained in the text.

Such radiative processes may be lethal for models attempting to produce positrons without overproducing antiprotons due to the subsequent hadronization of the radiated gauge bosons. Given that electroweak bremsstrahlung is the dominant annihilation channel for the DM models under consideration, and both W and Z decay to hadrons with a branching ratio of approximately 70%, a large hadronic component is unavoidable. Importantly in the context of recent cosmic ray data, there will be sizable antiproton production. We also note that dark matter searches triggering on anti-deuterons will find a sample in the W- and Z-bremsstrahlung processes. The Aleph experiment has measured an anti-deuteron production rate of $5.9 \pm 1.9 \times 10^{-6}$ anti-deuterons per hadronic decay of the Z [39]. We expect the rate for anti-deuteron production in W-decay to be similar.

Even for models which do not suffer a suppression of the lowest order process, we see that it is impossible to have purely leptonic annihilation products, including "leptophilic" models in which the dark matter has direct couplings only to leptons. In a broader context the results presented here show the importance that may be played by electroweak bremsstrahlung in future searches of indirect dark matter detection. For any DM model for which electroweak bremsstrahlung makes an important contribution to observable fluxes, there will be large, correlated fluxes of $e^\pm$, neutrinos, hadrons and gamma rays. We will explore the detection of these signals in a future article [40].

ACKNOWLEDGMENTS

We thank Sheldon Campbell, Bhaskar Dutta, Sourish Dutta, Haim Goldberg, Lawrence Krauss, Danny Marfatia, Yudi Santoso and Nick Setzer for helpful discussions. NFB was supported by the Australian Research Council, TDJ was supported by the Commonwealth of Australia, and TJW and JBD were supported in part by U.S. DoE grant DE–FG05–85ER40226. TJW benefited from a AvHumboldt Senior Research Award and hospitality at MPIK (Heidelberg), MPIH (Munich), U. Dortmund and the Aspen Center for Physics.

Appendix A: Fundamentals of Fierzing

In this paper we have made use of standard Fierz transformations, helicity-basis Fierz transformations, and generalizations of the two. In this Appendix, we derive these transformations. The procedure for standard Fierz transformation can be found in, e.g., [25], while more general Fierz transformations are laid down in [24]. The starting point is to define a basis $\{\Gamma^B\}$ and a dual basis $\{\Gamma_B\}$, each spanning 4×4 matrices over the complex number field $\mathcal{C}$, such that an orthogonality relation holds. The standard Fierz transformation uses the "hermitian" bases

$$\{\Gamma^B\} = \{\mathbb{1}, i\gamma_5, \gamma^\mu, \gamma_5\gamma^\mu, \sigma^{\mu\nu}\}\,, \quad \text{and}$$
$$\{\Gamma_B\} = \{\mathbb{1}, (-i\gamma_5), \gamma_\mu, (-\gamma_5\gamma_\mu), \frac{1}{2}\sigma_{\mu\nu}\}\,, \quad (A1)$$

respectively. Because of their Lorentz and parity transformation properties, these basis matrices and their duals are often labeled as S and $\tilde{S}$ (scalars), P and $\tilde{P}$ (pseudoscalars), V and $\tilde{V}$ (vectors, four for V, four for $\tilde{V}$), A and $\tilde{A}$ (axial vector, four for A, four for $\tilde{A}$), and T and $\tilde{T}$ (antisymmetric tensor, six for T, six for $\tilde{T}$). As usual, spacetime indices are lowered with the Minkowski metric, $\gamma_5 = \gamma^5 = i\gamma^0\gamma^1\gamma^2\gamma^3$, $\sigma^{\mu\nu} \equiv \frac{i}{2}[\gamma^\mu, \gamma^\nu]$, (and $\gamma^5\sigma^{\mu\nu} = \frac{i}{2}\epsilon^{\mu\nu\alpha\beta}\sigma_{\alpha\beta}$). Note the change of sign between the the basis and dual for the P and A matrices. The bases are "hermitian" in that $\gamma^0\,\Gamma_B^\dagger\gamma^0 = \Gamma_B$, so that the associated Dirac bilinears satisfy $[\bar\Psi_1\Gamma^B\Psi_2]^\dagger = \bar\Psi_2\Gamma^B\Psi_1$ and $[\bar\Psi_1\Gamma_B\Psi_2]^\dagger = \bar\Psi_2\Gamma_B\Psi_1$. Importantly, we have $\Gamma_B = (\Gamma^B)^{-1}$ in the sense of the accompanying orthogonality relation

$$Tr\,[\Gamma_C\,\Gamma^B\,] = 4\,\delta_C^B\,, \quad B,\,C = 1,\ldots,16\,. \tag{A2}$$

Note that the factor of $\frac{1}{2}$ in the definition of $\tilde T = \frac{1}{2}\sigma_{\mu\nu}$ (but not in $T = \sigma^{\mu\nu}$) provides the normalization required by Eq. (A2):

$$Tr\,[\Gamma_B\,\Gamma^B]_{(\text{nosum})} = \sum_C Tr\,[\Gamma_C\,\Gamma^B] = 4\,. \tag{A3}$$

The orthogonality relation allows us to expand any 4×4 complex matrix X in terms of the basis as

$$\begin{aligned} \mathrm{X} &= \mathrm{X}_B\,\Gamma^B = \mathrm{X}^B\,\Gamma_B\,, \quad \text{with} \\ \mathrm{X}_B &= \frac{1}{4}Tr\,[\,\mathrm{X}\,\Gamma_B\,]\,,\ \text{and}\ \mathrm{X}^B = \frac{1}{4}Tr\,[\,\mathrm{X}\,\Gamma^B\,]\,, \\ \text{i.e.,}\quad \mathrm{X} &= \frac{1}{4}\,Tr\,[\mathrm{X}\,\Gamma^B]\,\Gamma_B = \frac{1}{4}\,Tr\,[\mathrm{X}\,\Gamma_B]\,\Gamma^B\,. \end{aligned} \tag{A4}$$

One readily finds that the particular matrix element $(\mathrm{X})_{ab}$ satisfies

$$(\mathrm{X})_{cd}\,\delta_{db}\,\delta_{ac} = \frac{1}{4}\,[(\mathrm{X})_{cd}\,(\Gamma_B)_{dc}\,]\,(\Gamma^B)_{ab}\,. \tag{A5}$$

Since each element $(\mathrm{X})_{cd}$ is arbitrary, Eq. (A5) is equivalent to a completeness relation

$$(\mathbb{1})\,[\mathbb{1}] = \frac{1}{4}\,(\Gamma_B\,]\,[\Gamma^B\,) = \frac{1}{4}\,(\Gamma^B\,]\,[\Gamma_B\,)\,, \tag{A6}$$

where we have adopted Takahashi's notation [26] where matrix indices are replaced by parentheses $(\cdots)$ and brackets $[\cdots]$, in an obvious way. Thus, any 4×4 matrices X and Y may be expressed as

$$\begin{aligned} (\mathrm{X})\,[\mathrm{Y}] &= (\mathrm{X}\mathbb{1})\ [\mathbb{1}\mathrm{Y}] = \frac{1}{4}\,(\mathrm{X}\,\Gamma^B\,\mathrm{Y}\,]\ [\,\Gamma_B\,) \\ &= \frac{1}{4^2}\,Tr\,[\mathrm{X}\,\Gamma^B\,\mathrm{Y}\,\Gamma_C]\ (\Gamma^C\,]\ [\Gamma_B\,)\,. \end{aligned} \tag{A7}$$

This equation is presented as Eq. (6) in the main text. Alternatively, we may express any 4×4 matrices X and Y as

$$\begin{aligned} (\mathrm{X})\,[\mathrm{Y}] &= (\mathrm{X}\mathbb{1})\ [Y\mathbb{1}] = \frac{1}{4}\,(\mathrm{X}\,\Gamma^B]\ [Y\,\Gamma_B\,) \\ &= \frac{1}{4^3}\,Tr\,[\mathrm{X}\,\Gamma^B\,\Gamma_C]\ Tr\,[\mathrm{Y}\,\Gamma_B\,\Gamma^D]\ (\Gamma^C\,]\ [\Gamma_D\,)\,. \end{aligned} \tag{A8}$$

The RHS's of Eqs. (A7) and (A8) offer two useful options for Fierzing matrices. The first option sandwiches both LHS matrices into one of the two spinor bilinears, and ultimately into a single long trace. The second option sandwiches each LHS matrix into a separate spinor bilinear, and ultimately into separate trace factors. Eq. (A7) seems to be more useful than (A8). One use we will make of Eq. (A7) will be to express chiral vertices in terms of Fierzed standard vertices. But first we reproduce the standard Fierz transformation rules by setting $\mathrm{X} = \Gamma^D$ and $\mathrm{Y} = \Gamma_E$ in Eq. (A7), to wit:

$$(\Gamma^D)\,[\Gamma_E] = \frac{1}{4^2}\,Tr\,[\Gamma^D\,\Gamma^B\,\Gamma_E\,\Gamma_C]\,(\Gamma^C]\,[\Gamma_B)\,. \tag{A9}$$

(An additional minus sign arises if the matrices are sandwiched between anticommuting field operators, rather than between Dirac spinors.) Evaluation of the trace in Eq. (A9) for the various choices of (B, C) leads to the oft-quoted result [25]

$$\begin{pmatrix} (S)\ [\tilde S] \\ (V)\ [\tilde V] \\ (T)\ [\tilde T] \\ (A)\ [\tilde A] \\ (P)\ [\tilde P] \end{pmatrix} = \frac{1}{4}\begin{pmatrix} 1 & 1 & 1 & 1 & 1 \\ 4 & -2 & 0 & 2 & -4 \\ 6 & 0 & -2 & 0 & 6 \\ 4 & 2 & 0 & -2 & -4 \\ 1 & -1 & 1 & -1 & 1 \end{pmatrix}\begin{pmatrix} (S]\ [\tilde S) \\ (V]\ [\tilde V) \\ (T]\ [\tilde T) \\ (A]\ [\tilde A) \\ (P]\ [\tilde P) \end{pmatrix}. \tag{A10}$$

More relevant for us, as will be seen, is the ordering P, S, A, V, T, which leads to a Fierz matrix obtained from the one above with the swapping of matrix indices $1 \to 2 \to 4 \to 3 \to 5 \to 1$. The result is

$$\begin{pmatrix} (P)\ [\tilde P] \\ (S)\ [\tilde S] \\ (A)\ [\tilde A] \\ (V)\ [\tilde V] \\ (T)\ [\tilde T] \end{pmatrix} = \frac{1}{4}\begin{pmatrix} 1 & 1 & -1 & -1 & 1 \\ 1 & 1 & 1 & 1 & 1 \\ -4 & 4 & -2 & 2 & 0 \\ -4 & 4 & 2 & -2 & 0 \\ 6 & 6 & 0 & 0 & -2 \end{pmatrix}\begin{pmatrix} (P]\ [\tilde P) \\ (S]\ [\tilde S) \\ (A]\ [\tilde A) \\ (V]\ [\tilde V) \\ (T]\ [\tilde T) \end{pmatrix}. \tag{A11}$$

(The zeroes make it clear that Fierzing induces no coupling between tensor interactions and vector and axial vector interactions.) As an example of how to read this matrix,

$$(A)\ [\tilde A] = -(P]\ [\tilde P) + (S]\ [\tilde S) - \frac{1}{2}(A]\ [\tilde A) + \frac{1}{2}(V]\ [\tilde V), \tag{A12}$$

or, multiplying by spinors and giving the explicit forms of the gamma-matrices,

$$\begin{aligned} &(\overline{u}\gamma_5\gamma^\mu u)\ \ (\overline{v}(-\gamma_5\gamma_\mu)v) \\ &\quad = -\,(\overline{u}i\gamma_5 v)\ \ (\overline{v}\,(-i\gamma_5)\,u) + (\overline{u}v)\ \ (\overline{v}u) \\ &\quad -\frac{1}{2}\,(\overline{u}\gamma_5\gamma^\mu v)\ \ (\overline{v}\,(-\gamma_5\gamma_\mu)\,u) + \frac{1}{2}\,(\overline{u}\gamma^\mu v)\ \ (\overline{v}\gamma_\mu u)\,. \end{aligned} \tag{A13}$$

The Fierz matrix M for the standard basis is nonsingular, and hence has five nonzero eigenvalues λ_j. Since two swaps of Dirac indices returns the indices to their original order, the matrix is idempotent, with $M^2 = \mathbb{1}$, or equivalently, $M^{-1} = M$. Accordingly, the five eigenvalues satisfy $\lambda_j^2 = 1$, so individual eigenvalues must be $\lambda_j = \pm 1$. Also, the corresponding eigenvectors are invariant under the interchange of two Dirac indices. In

TABLE II. Fierz-invariant combinations in the standard basis.

Fierz-invariant combination	eigenvalue
$3\,(S\otimes\tilde{S}+P\otimes\tilde{P})+T\otimes\tilde{T}$	$+1$
$2\,(S\otimes\tilde{S}-P\otimes\tilde{P})+(V\otimes\tilde{V}+A\otimes\tilde{A})$	$+1$
$V\otimes\tilde{V}-A\otimes\tilde{A}$	-1
$S\otimes\tilde{S}+P\otimes\tilde{P}-T\otimes\tilde{T}$	-1
$2\,(S\otimes\tilde{S}-P\otimes\tilde{P})-(V\otimes\tilde{V}+A\otimes\tilde{A})$	-1

Table (II) we list the eigenvalues and "Fierz-invariant" eigenvectors.

Helicity projection operators are often present in theories where the DM couple to the $SU(2)$ lepton doublet, so it is worth considering Fierz transformations in the more convenient chiral basis.

One derivation of chiral Fierz transformations utilizes the following chiral bases (hatted) [24]:

$$\{\hat{\Gamma}^B\}=\{P_R,\,P_L,\,P_R\gamma^\mu,\,P_L\gamma^\mu,\,\frac{1}{2}\sigma^{\mu\nu}\}\,,\quad \text{and}$$
$$\{\hat{\Gamma}_B\}=\{P_R,\,P_L,\,P_L\gamma_\mu,\,P_R\gamma_\mu,\,\frac{1}{2}\,\sigma_{\mu\nu}\}\,,\qquad \text{(A14)}$$

where $P_R\equiv\frac{1}{2}(1+\gamma_5)$ and $P_L\equiv\frac{1}{2}(1-\gamma_5)$ are the usual helicity projectors. The orthogonality property between the chiral basis and its dual is

$$Tr\,[\hat{\Gamma}_C\,\hat{\Gamma}^B\,]=2\,\delta^B_C\,,\quad B,\,C=1,\ldots,16\,,\qquad \text{(A15)}$$

which implies the normalization

$$Tr\,[\hat{\Gamma}_B\,\hat{\Gamma}^B]_{(\text{no sum})}=\sum_C Tr\,[\hat{\Gamma}_C\,\hat{\Gamma}^B]=2\,.\qquad \text{(A16)}$$

Notice that because $\{\gamma_5,\gamma^\mu\}=0$, the dual of $P_R\gamma^\mu$ is $P_L\gamma_\mu$, and the dual of $P_L\gamma^\mu$ is $P_R\gamma_\mu$. Notice also that the normalization for the chiral bases necessitates factors of $\frac{1}{2}$ in both $\hat{T}=\frac{1}{2}\sigma^{\mu\nu}$ and $\tilde{\hat{T}}=\frac{1}{2}\sigma_{\mu\nu}$, in contrast to the tensor elements of the standard bases, given in Eq. (A1).

In the chiral basis, one is led to a general expansion

$$\mathrm{X}=\frac{1}{2}\,Tr\,[\mathrm{X}\,\hat{\Gamma}^B]\,\hat{\Gamma}_B=\frac{1}{2}\,Tr\,[\mathrm{X}\,\hat{\Gamma}_B]\,\hat{\Gamma}^B\,,\qquad \text{(A17)}$$

and to a completeness relation

$$(\mathbb{1})\,[\mathbb{1}]=\frac{1}{2}\,(\hat{\Gamma}_B\,]\,[\hat{\Gamma}^B\,)=\frac{1}{2}\,(\hat{\Gamma}^B\,]\,[\hat{\Gamma}_B\,)\,.\qquad \text{(A18)}$$

Thus, any 4×4 matrices X and Y may be expressed as

$$(\mathrm{X})\,[\mathrm{Y}]=(\mathrm{X}\mathbb{1})\,[\mathbb{1}\mathrm{Y}]=\frac{1}{2}(\mathrm{X}\,\hat{\Gamma}_B\,\mathrm{Y}\,]\,[\,\hat{\Gamma}^B\,)$$
$$=\frac{1}{4}\,Tr\,[\mathrm{X}\,\hat{\Gamma}^C\,\mathrm{Y}\,\hat{\Gamma}_B]\;(\hat{\Gamma}^B\,]\,[\hat{\Gamma}_C\,)\,.\qquad \text{(A19)}$$

Substituting $\mathrm{X}=\hat{\Gamma}^D$ and $\mathrm{Y}=\hat{\Gamma}_E$ into Eq. (A19), one gets

$$(\hat{\Gamma}^D)\,[\hat{\Gamma}_E]=\frac{1}{4}\,Tr\,[\hat{\Gamma}^D\,\hat{\Gamma}^C\,\hat{\Gamma}_E\,\hat{\Gamma}_B]\;(\hat{\Gamma}^B]\;[\hat{\Gamma}_C)\,.\qquad \text{(A20)}$$

TABLE III. Fierz-invariant combinations in the chiral basis.

Fierz-invariant combination	eigenvalue
$3\,(P_R\otimes P_R+P_L\otimes P_L)+\hat{T}\otimes\tilde{\hat{T}}$	$+1$
$2\,P_R\otimes P_L+P_R\gamma^\mu\otimes P_L\gamma_\mu$	$+1$
$2\,P_L\otimes P_R+P_L\gamma^\mu\otimes P_R\gamma_\mu$	$+1$
$P_R\otimes P_R+P_L\otimes P_L-\hat{T}\otimes\tilde{\hat{T}}$	-1
$2\,P_R\otimes P_L-P_R\gamma^\mu\otimes P_L\gamma_\mu$	-1
$2\,P_L\otimes P_R-P_L\gamma^\mu\otimes P_R\gamma_\mu$	-1
$P_R\gamma^\mu\otimes P_R\gamma_\mu$	-1
$P_L\gamma^\mu\otimes P_L\gamma_\mu$	-1

Evaluating the trace in Eq. (2) leads to the chiral-basis analog of (A10) or (A11), presented in Eq. (3) of the main text.

As a check, we note that the matrix M in Eq. (3) is idempotent, $M^2=\mathbb{1}$, as it must be. The eigenvalues are therefore ±1. Eigenvalues and Fierz-invariant eigenvectors for the chiral basis are given in Table (III). The final two eigenvectors in the Table simply express again the invariance of $V\pm A$ interactions under Fierz-transposition of Dirac indices. This invariance is also evident in the diagonal nature of the bottom two rows of the matrix Eq. (3).

One may instead want the Fierz transformation that takes chiral bilinears to standard bilinears. Since models are typically formulated in terms of chiral fermions, a projection onto standard s-channel bilinears would be well- suited for a partial wave analysis. Because different partial waves do not interfere with one another, the calculation simplifies in terms of s-channel partial waves.

Setting $\mathrm{X}=\hat{\Gamma}^D$ and $\mathrm{Y}=\hat{\Gamma}_E$ in Eq. (A7), we readily get

$$(\hat{\Gamma}^D)\,[\hat{\Gamma}_E]=\frac{1}{4^2}\,Tr\,[\hat{\Gamma}^D\,\Gamma^B\,\hat{\Gamma}_E\,\Gamma_C]\,(\Gamma^C]\,[\Gamma_B)\,.\qquad \text{(A21)}$$

We (should) get the same result by resolving the RHS vector in Eq. (3) into standard basis matrices. The result is

$$\begin{pmatrix} (P_R)\ [P_R] \\ (P_L)\ [P_L] \\ (P_R\gamma^\mu)\ [P_L\gamma_\mu] \\ (P_L\gamma^\mu)\ [P_R\gamma_\mu] \\ (\hat{T})\ [\hat{T}] \\ (\gamma_5\hat{T})\ [\hat{T}] \\ (P_R)\ [P_L] \\ (P_L)\ [P_R] \\ (P_R\gamma^\mu)\ [P_R\gamma_\mu] \\ (P_L\gamma^\mu)\ [P_L\gamma_\mu] \end{pmatrix} = \frac{1}{8} \left(\begin{array}{rrrrrr|rrrr} 1 & 1 & 1 & 1 & 1 & 1 & 0 & 0 & 0 & 0 \\ 1 & 1 & -1 & -1 & 1 & -1 & 0 & 0 & 0 & 0 \\ 4 & -4 & 4 & -4 & 0 & 0 & 0 & 0 & 0 & 0 \\ 4 & -4 & -4 & 4 & 0 & 0 & 0 & 0 & 0 & 0 \\ 6 & 6 & 0 & 0 & -2 & 0 & 0 & 0 & 0 & 0 \\ 0 & 0 & 6 & 6 & 0 & 2 & 0 & 0 & 0 & 0 \\ \hline 0 & 0 & 0 & 0 & 0 & 0 & 1 & -1 & 1 & -1 \\ 0 & 0 & 0 & 0 & 0 & 0 & 1 & -1 & -1 & 1 \\ 0 & 0 & 0 & 0 & 0 & 0 & -2 & -2 & -2 & -2 \\ 0 & 0 & 0 & 0 & 0 & 0 & -2 & -2 & 2 & 2 \end{array}\right) \begin{pmatrix} (\mathbb{1}]\ [\mathbb{1}) \\ (\gamma_5]\ [\gamma_5) \\ (\gamma_5]\ [\mathbb{1}) \\ (\mathbb{1}]\ [\gamma_5) \\ (T]\ [\tilde{T}) \\ (\gamma_5 T]\ [\tilde{T}) \\ (\gamma^\mu]\ [\gamma_\mu) \\ (\gamma_5\gamma^\mu]\ [\gamma_5\gamma_\mu) \\ (\gamma_5\gamma^\mu]\ [\gamma_\mu) \\ (\gamma^\mu]\ [\gamma_5\gamma_\mu) \end{pmatrix} \tag{A22}$$

All relations are invariant under the simultaneous interchanges $P_R \leftrightarrow P_L$ and $\gamma_5 \to -\gamma_5$. The matrix in (A22), relating two different bases, is not idempotent. In fact, it is singular.

Appendix B: Cancellation of Vector and Tensor Amplitudes for Majorana Fermions

Majorana particles are invariants under charge conjugation $\mathcal{C}$. Accordingly, the Majorana field creates and annihilates the same particle. This implies that for each t-channel diagram, there is an accompanying u-channel diagram, obtained by interchanging the momentum and spin of the two Majorana fermions. The relative sign between the t- and u-channel amplitudes is -1 in accord with Fermi statistics. For example, consider the Fierzed (i.e., s-channel) bilinear for χ-annihilation: $\bar{v}(k_1, s_1)\Gamma_B u(k_2, s_2)$. The associated Fierzed bilinear from the ($k_1 \leftrightarrow k_2$)-exchange graph, with its relative minus sign, is $-\bar{v}(k_2, s_2)\Gamma_B u(k_1, s_1)$. Constraints relating the four-component Dirac spinors to their underlying two-component Majorana spinors must be imposed. These constraints, any one of which implies the other three, are

$$\begin{aligned} u(p,s) &= C\bar{v}^T(p,s)\,, \quad \bar{u}(p,s) = -v^T(p,s)C^{-1}\,, \\ v(p,s) &= C\bar{u}^T(p,s)\,, \quad \bar{v}(p,s) = -u^T(p,s)C^{-1}\,. \end{aligned} \tag{B1}$$

Here, C is the charge conjugation matrix. These Majorana conditions on the spinors allow us to rewrite the exchange bilinear as (suppressing spin labels for brevity of notation)

$$\begin{aligned} -\bar{v}(k_2)\Gamma_B u(k_1)) &= u^T(k_2)C^{-1}\Gamma_B C\bar{v}^T(k_1) \\ &= \left[\bar{v}(k_1)(C^{-1}\Gamma_B C)^T u(k_2)\right]^T \\ &= \bar{v}(k_1)(\eta_B\Gamma_B)u(k_2)\,. \end{aligned} \tag{B2}$$

For the final equality, we have used (i) the fact that the transpose symbol can be dropped from a number, and (ii) the identity $(C^{-1}\Gamma_B C)^T = (\eta_B(\Gamma_B)^T)^T = \eta_B\Gamma_B$, where $\eta_B = +1$ for $\Gamma =$ scalar, pseudoscalar, axial vector, and $\eta_B = -1$ for $\Gamma =$ vector or tensor.

In the Four-Fermi or heavy propagator limit, where the differing momenta in the t- and u-channel propagators can be ignored, one obtains an elegant simplification. Subtracting the u-channel amplitude from the t-channel amplitude, one arrives at the weighting factor $(1 + \eta_B)$, which is two for S, P, and A couplings, and zero for V and T couplings. Thus, we must drop V and T couplings appearing in the Fierzed bilinears of the χ-current. What this means for the model under discussion is that after Fierzing, only the axial vector coupling of the χ-current remains, and the factor of $1+\eta_A = 2$ is multiplied by the (7-8)-element $= \frac{1}{2}$ in the Fierz matrix of Eq. (3) to give a net weight of 1.

Appendix C: Non-Relativistic and Extreme-Relativistic Limits of Fermion Bilinears

We work in the chiral representation of the Dirac algebra, and we follow the notation of [27]. Accordingly,

$$\gamma_0 = \begin{pmatrix} 0 & \mathbb{1} \\ \mathbb{1} & 0 \end{pmatrix}\,, \quad \vec{\gamma} = \begin{pmatrix} 0 & \vec{\sigma} \\ -\vec{\sigma} & 0 \end{pmatrix}\,, \quad \gamma_5 = \begin{pmatrix} -\mathbb{1} & 0 \\ 0 & \mathbb{1} \end{pmatrix}\,. \tag{C1}$$

The rest-frame four-spinor is

$$u(\vec{p} = 0) = \sqrt{M}\begin{pmatrix} \xi \\ \xi \end{pmatrix}\,, \tag{C2}$$

where ξ is a two-dimensional spinor. The spinor with arbitrary momentum is obtained by boosting. One gets

$$u(p) = \begin{pmatrix} \sqrt{p\cdot\sigma}\,\xi \\ \sqrt{p\cdot\overline{\sigma}}\,\xi \end{pmatrix}\,, \tag{C3}$$

where $\sigma \equiv (1, \vec{\sigma})$ and $\overline{\sigma} \equiv (1, -\vec{\sigma})$.

In a standard fashion, we choose the up and down spin eigenstates of σ_3 as the basis for the two-spinors. These basis two-spinors are

$$\xi_+ \equiv \begin{pmatrix} 1 \\ 0 \end{pmatrix}\,, \quad \xi_- \equiv \begin{pmatrix} 0 \\ 1 \end{pmatrix}\,. \tag{C4}$$

In terms of the chosen basis, we have for the NR u-spinors,

$$u_\pm \xrightarrow{NR} \sqrt{M} \begin{pmatrix} \xi_\pm \\ \xi_\pm \end{pmatrix} . \tag{C5}$$

We get the ER limit of the u-spinors from Eq. (C3). After a bit of algebra, one finds

$$u_+ \xrightarrow{ER} \sqrt{2E} \begin{pmatrix} 0 \\ 0 \\ \xi_+ \end{pmatrix} , \quad u_- \xrightarrow{ER} \sqrt{2E} \begin{pmatrix} \xi_- \\ 0 \\ 0 \end{pmatrix} . \tag{C6}$$

The arbitrary v-spinor is given by

$$v(p) = \begin{pmatrix} \sqrt{p\cdot\sigma}\,\eta \\ \\ -\sqrt{p\cdot\overline{\sigma}}\,\eta \end{pmatrix} . \tag{C7}$$

In the Dirac bilinear the two-spinor η is independent of the two-spinor xi, and so it is given an independent name, η. However, the basis $\eta^\pm$ remains $\xi^\pm$ as defined above. It is the minus sign in the lower components of v relative to the upper components that distinguishes v in eq. (C7) from u in eq. (C3) in a fundamental way. After a small amount of algebra, one finds the limits

$$v_\pm \xrightarrow{NR} v_\pm(\vec{p}=0) = \sqrt{M} \begin{pmatrix} \eta_\pm \\ -\eta_\pm \end{pmatrix} , \tag{C8}$$

and

$$v_+ \xrightarrow{ER} \sqrt{2E} \begin{pmatrix} 0 \\ 0 \\ -\eta_+ \end{pmatrix} , \quad v_- \xrightarrow{ER} \sqrt{2E} \begin{pmatrix} \eta_- \\ 0 \\ 0 \end{pmatrix} . \tag{C9}$$

Finally, we apply the above to determine the values of Dirac bilinears in the NR and ER limits. The $\bar{u} \equiv u^\dagger\,\gamma_0$ and $\bar{v} \equiv v^\dagger\,\gamma_0$ conjugate spinors are are easily found from the u and v spinors. We let Γ denote any of the hermitian basis Dirac-matrices $\{\mathbb{1},\ i\,\gamma_5,\ \gamma^\mu,\ \gamma_5\,\gamma^\mu,\ \sigma^{\mu\nu}\}$. Then, the NR limit of $\bar{u}(p_1)\,\Gamma\,v(p_2)$ is just

$$\bar{u}(p_1)\,\Gamma\,v(p_2) \xrightarrow{NR} M \left[(\xi_1,\ \xi_1)\ \Gamma \begin{pmatrix} \eta_2 \\ -\eta_2 \end{pmatrix} \right] . \tag{C10}$$

Non-relativistic results for the various choices of basis Γ's and spin combinations are listed in Table I of the text.

To give a succinct formula for the ER limit of $\bar{u}(p_1)\,\Gamma\,v(p_2)$, we take $\hat{p}_1 = -\hat{p}_2 = \hat{3}$, i.e. we work in a frame where $\hat{p}_1$ and $\hat{p}_2$ are collinear, and we quantize the spin along this collinear axis. The result is

$$\bar{u}(p_1)\,\Gamma\,v(p_2) \xrightarrow{ER} \sqrt{4E_1E_2} \left[\xi_1 \ \ (\Lambda_+,\ \Lambda_-)\,\Gamma \begin{pmatrix} \Lambda_+ \\ -\Lambda_- \end{pmatrix} \eta_2 \right] , \tag{C11}$$

where the matrices $\Lambda_\pm$ are just up and down spin projectors along the quantization axis $\hat{3}$:

$$\lambda_+ = \begin{pmatrix} 1 & 0 \\ 0 & 0 \end{pmatrix} , \quad \Lambda_- = \begin{pmatrix} 0 & 0 \\ 0 & 1 \end{pmatrix} . \tag{C12}$$

Extreme-relativistic results for the various choices of basis Γ's and spin combinations are listed in Table I of the text.

Appendix D: Full Cross Section Results

We present here the full results of the cross section calculations for the process $\chi\chi \to \mathrm{e}^\mp \overset{(-)}{\nu} W^\pm$, including terms of all orders in M_χ. In Section IV we presented only the leading order terms, which dominate in the large M_χ limit. For M_χ not too much heavier than M_W, it is important to retain sub-leading terms.

The total cross section for $\chi\chi \to \mathrm{e}^\mp \overset{(-)}{\nu} W^\pm$ is given by

$$\begin{aligned} v\,\sigma_{\mathrm{e}^+\nu W^-} = & \frac{g^2 f^4}{2^{13} M_W^2 M_\eta^4 \pi^3} \Bigg\{ \left(\frac{7}{32}\frac{M_W^8}{M_\chi^4} - \frac{7}{9}\frac{M_W^6}{M_\chi^2} + 4M_W^4 - 16M_W^2M_\chi^2 - \frac{56}{9}M_\chi^4 \right) \\ & + \ln\left[\frac{4M_\chi^2}{M_W^2}\right] \left(\frac{1}{16}\frac{M_W^8}{M_\chi^4} + \frac{4}{3}\frac{M_W^6}{M_\chi^2} - 2M_W^4 + 16M_W^2M_\chi^2 + \frac{16}{3}M_\chi^4 + 8M_W^2\left(M_W^2+2M_\chi^2\right)\ln\left[\frac{2M_WM_\chi}{M_W^2+4M_\chi^2}\right] \right) \\ & + 8M_W^2\left(M_W^2+2M_\chi^2\right)\left(\mathrm{Li}_2\left[\frac{4M_\chi^2}{M_W^2+4M_\chi^2}\right] - \mathrm{Li}_2\left[\frac{M_W^2}{M_W^2+4M_\chi^2}\right] \right) + \mathcal{O}(v^2, M_\eta^{-2}, m_\ell^2) \Bigg\}. \end{aligned} \tag{D1}$$

The W energy spectrum is

$$\frac{v\,d\sigma_{\mathrm{e}^+\nu W^-}}{dE_W} = \frac{g^2 f^4}{512 E_W M_W^2 M_\eta^4 \pi^3}\Bigg\{2E_W\sqrt{E_W^2 - M_W^2}\left(M_W^2 - 6E_W^2 + 8E_W M_\chi - 2M_\chi^2\right) \tag{D2}$$

$$+ \left(4E_W^4 - 8E_W^3 M_\chi + (2E_W^2 - M_W^2)\left(2M_\chi^2 + M_W^2\right)\right)\ln\left[\frac{E_W + \sqrt{E_W^2 - M_W^2}}{E_W - \sqrt{E_W^2 - M_W^2}}\right] + \mathcal{O}(v^2, M_\eta^{-2}, m_\ell^2)\Bigg\},$$

while the lepton spectrum (for either the charged lepton or the neutrino) is

$$\frac{v\,d\sigma_{\mathrm{e}^+\nu W^-}}{dE_\ell} = \frac{g^2 f^4}{2^{18} M_\eta^4 (M_\chi - E_e)\pi^3}\Bigg\{\frac{E_e\left(4(M_\chi - E_e)M_\chi - M_W^2\right)}{M_W^2 M_\chi^4\left(M_W^2 + 4E_e M_\chi\right)(M_\chi - E_e)^4}$$

$$\times\Bigg(7\times 2^8 E_e^7 M_W^4 + 2^8 E_e^6 M_\chi^3\left(M_W^2 - \frac{139}{3}M_\chi^2\right) - 2^5 E_e^5 M_\chi^2\left(M_W^4 + \frac{146}{3}M_\chi^2 M_W^2 - 984 M_\chi^4\right)$$

$$- 2^4 E_e^4 M_\chi\left(M_W^6 - 13 M_W^4 M_\chi^2 - 232 M_\chi^4 M_W^2 + 2704 M_\chi^6\right)$$

$$+ E_e^3\left(-M_W^8 + \frac{164}{3}M_W^6 M_\chi^2 - 560 M_W^4 M_\chi^4 - 4672 M_\chi^6 M_W^2 + \frac{191\times 2^9}{3}M_\chi^8\right)$$

$$+ 8E_e^2 M_\chi\left(\frac{1}{3}M_W^8 - 6M_W^6 M_\chi^2 + 116 M_W^4 M_\chi^4 + \frac{1376}{3}M_\chi^6 M_W^2 - 1600 M_\chi^8\right)$$

$$- 2E_e M_\chi^2\left(M_W^8 M_\chi^2 - 4M_W^6 M_\chi^2 + 400 M_W^4 M_\chi^4 + 960 M_\chi^6 M_W^2 - 2^{10} M_\chi^8\right) + 2^8 M_\chi^3\left(M_W^2 + 2M_\chi^2\right)\Bigg)$$

$$+ 2^8\left(2M_\chi^2 + M_W^2 - \frac{4E_e^2(M_\chi - E_e)^2}{M_W^2}\right)\ln\left[\frac{M_W^2 M_\chi}{(M_\chi - E_e)\left(M_W^2 + 4E_e M_\chi\right)}\right]\Bigg\} + \mathcal{O}(v^2, M_\eta^{-2}, m_\ell^2). \tag{D3}$$

Appendix E: Approximate Spectrum for Boosted *W* Decay Products

If any possible polarization of the produced W is neglected, then a simple calculation results for the spectra of the finals state particles from W decay. The lab frame spectra of the decay product (of type or "flavor" F) depends on a one-dimensional convolution of the isotropic spectrum in the W rest frame (RF energy E'), $\frac{dN_F}{dE'_{F'}}$, with the W spectrum in the lab frame, $\frac{dN}{dE_W}$. We now develop this convolution.

Given the energy distribution $dN_W/d\gamma$ of produced W's (with $\gamma = E_W/M_W$), and the energy distribution dN_F/dE'_F of decay particle F in the W rest frame, normalized to the multiplicity of F per W decay (i.e., there is a branching ratio $W \to F$ multiplier implicit in dN_F/dE'_F) and assumed to be isotropic,[4] one gets the spectrum dN_F/dE_F of particle F in the lab via:

$$\frac{dN_F(E)}{dE} = \int_{-1}^{1}\frac{d\cos\theta'}{2}\int d\gamma\frac{dN_W}{d\gamma} \times\int dE'\,\frac{dN_F}{dE'}\;\delta(E - [\gamma E' + \beta\gamma p'\cos\theta'])\,, \tag{E1}$$

with $p' = \sqrt{E'^2 - m_F^2}$, $\beta\gamma = \sqrt{\gamma^2 - 1}$. The $\cos\theta'$ integral is easily done, and one gets

$$\frac{dN_F(E)}{dE} = \frac{1}{2}\int_1^\infty \frac{d\gamma}{\sqrt{\gamma^2-1}}\frac{dN_W}{d\gamma}\int_{E'_-}^{E'_+}\frac{dE'}{p'}\,\frac{dN_F}{dE'}\,, \tag{E2}$$

with $E'_\pm = \gamma E \pm \beta\gamma p$. Equivalently, we get

$$\frac{dN_F(E)}{dE} = \frac{1}{2}\int_{m_F}^\infty \frac{dE'}{p'}\,\frac{dN_F}{dE'}\,,\int_{\gamma_-}^{\gamma_+}\frac{d\gamma}{\sqrt{\gamma^2-1}}\,\frac{dN_W}{d\gamma}\,, \tag{E3}$$

with $\gamma_\pm = (EE' \pm pp')/m_F^2$ and $p = \sqrt{E^2 - m_F^2}$. This formulation neglects interferences between identical particles produced in both the primary and secondary channels, if any.

As given, Eq. (E3) applies to any particle type in the W's final state. For example, it could be used to calculate the antiproton or antineutron spectrum from W production and decay, if the fragmentation functions for $W \to \bar{p}$ or $\bar{n}$, i.e. $f(x_{\bar{B}} \equiv 2E_{\bar{B}}/M_W)$ were input.

Here we perform a the convolution for the especially simple case of W decay to two massless particles, say ν_{e} and e. For massless leptons, we have

$$\frac{dN_\nu}{dE'} = \frac{dN_{\mathrm{e}}}{dE'} = BR(W \to \nu\mathrm{e})\,\delta(E' - \frac{1}{2}M_W)\,, \tag{E4}$$

with $\gamma_+ = (E_W/M_W)_{max} = (s + M_W^2)/2\sqrt{s}M_W \approx (4M_\chi^2 + M_W^2)/4M_\chi M_W$, and $\gamma_- = (4E^2 + M_W^2)/4EM_W$.

[4] If the W polarization is not neglected, then the W decay amplitude includes Wigner functions $d^1_{\mu_i\mu_f}(\theta)$, which introduce a linear $\cos\theta$ or $\sin\theta$ term into Eq. (E1).

The spectrum in the lab is given by Eq. (E3) becomes just

$$\frac{dN_\nu}{dE} = \frac{dN_e}{dE} = \frac{(BR)}{M_W} \int_{\gamma_-}^{\gamma_+} \frac{d\gamma}{\sqrt{\gamma^2-1}} \frac{dN_W}{d\gamma} \,. \tag{E5}$$

The W-spectrum shown in Fig. (3) is approximately half of an ellipse, suggesting the fit

$$\left(\frac{\ln\left(\frac{dN}{dx_W}\right) - \ln 0.07}{\ln 2.0 - \ln 0.07}\right)^2 + \left(\frac{x_W - 0.65}{0.50\,(1.01-0.29)}\right)^2 = 1\,, \tag{E6}$$

valid for $0.29 \lesssim x_W \lesssim 1.01$. Solving for dN/dx_W then gives

$$\frac{dN}{dx_W} = 0.07 \left(\frac{2.0}{0.07}\right)^{\sqrt{1-7.7\,(x_W-0.65)^2}} \,. \tag{E7}$$

Substituting into Eq. (E5) $\gamma = \frac{M_\chi}{M_W}\,x_W$, $\frac{dN}{d\gamma} = \frac{M_W}{M_\chi}\frac{dN}{dx_W}$, and $\frac{dN}{dx_W}$ given in Eq. (E7), we obtain the desired one-dimensional integral for the secondary lepton spectrum, per W:

$$\frac{dN_\nu(x_\ell)}{dx_\ell} = 0.07\,(BR) \int_{x_-}^{x_+} \frac{dx_W}{\sqrt{x_W^2 - \left(\frac{M_W}{M_\chi}\right)^2}} \times \left(\frac{2.0}{0.07}\right)^{\sqrt{1-7.7\,(x_W-0.65)^2}} \,. \tag{E8}$$

The integration limits are $x_+ = 1 + \frac{M_W^2}{4M_\chi^2}$, and $x_- = \left(x_\ell + \frac{M_W^2}{4x_\ell\, M_\chi^2}\right)$. The range of x_ℓ for the leptons from W decay is $[\frac{M_W^2}{4M_\chi^2},\ 1]$. The relevant branching ratios [41] are $BR(W \to \nu e) = 11\%$, $BR(Z \to \nu\bar{\nu}) = 6.7\%$, and $BR(Z \to \ell^+\ell^-) = 3.4\%$, each per single flavor mode, e, μ, or τ. We show the resulting lepton spectrum, without the BR factor, in Fig. (5).

[1] G. Jungman, M. Kamionkowski and K. Griest, Phys. Rept. **267**, 195 (1996).

[2] G. Bertone, D. Hooper and J. Silk, Phys. Rept. **405**, 279 (2005).

[3] L. Bergstrom, Rept. Prog. Phys. **63**, 793 (2000)

[4] L. Bergstrom, Phys. Lett. B **225**, 372 (1989);
R. Flores, K. A. Olive and S. Rudaz, Phys. Lett. B **232**, 377 (1989);
E. A. Baltz and L. Bergstrom, Phys. Rev. D **67**, 043516 (2003); [arXiv:hep-ph/0211325].
L. Bergstrom, T. Bringmann and J. Edsjo, Phys. Rev. D **78**, 103520 (2008) [arXiv:0808.3725 [astro-ph]];
V. Barger, Y. Gao, W. Y. Keung and D. Marfatia, Phys. Rev. D **80**, 063537 (2009) [arXiv:0906.3009 [hep-ph]].

[5] T. Bringmann, L. Bergstrom and J. Edsjo, JHEP **0801**, 049 (2008). [arXiv:0710.3169 [hep-ph]].

[6] V. Berezinsky, M. Kachelriess and S. Ostapchenko, Phys. Rev. Lett. **89**, 171802 (2002) [arXiv:hep-ph/0205218].

[7] M. Kachelriess and P. D. Serpico, Phys. Rev. D **76**, 063516 (2007) [arXiv:0707.0209 [hep-ph]].

[8] N. F. Bell, J. B. Dent, T. D. Jacques and T. J. Weiler, Phys. Rev. D **78**, 083540 (2008) [arXiv:0805.3423]. It has been pointed out in [11] that the bremsstrahlung rate presented in this paper is too low by a factor of $\frac{1}{4}$. This is so — Eq. (8) and the subsequent rate equations should be multiplied by 4.

[9] J. B. Dent, R. J. Scherrer and T. J. Weiler, Phys. Rev. D **78**, 063509 (2008) [arXiv:0806.0370 [astro-ph]].

[10] P. Ciafaloni and A. Urbano, arXiv:1001.3950 [hep-ph].

[11] M. Kachelriess, P. D. Serpico and M. A. Solberg, arXiv:0911.0001 [hep-ph].

[12] O. Adriani *et al.* [PAMELA Collaboration], Nature **458**, 607 (2009) [arXiv:0810.4995 [astro-ph]].

[13] O. Adriani *et al.*, Phys. Rev. Lett. **102**, 051101 (2009) [arXiv:0810.4994 [astro-ph]].

[14] O. Adriani *et al.* [PAMELA Collaboration], arXiv:1007.0821 [astro-ph.HE].

[15] A. A. Abdo *et al.* [The Fermi LAT Collaboration], Phys. Rev. Lett. **102**, 181101 (2009) [arXiv:0905.0025 [astro-ph.HE]].

[16] D. Hooper, P. Blasi and P. D. Serpico, JCAP **0901**, 025 (2009) [arXiv:0810.1527 [astro-ph]];
H. Yuksel, M. D. Kistler and T. Stanev, Phys. Rev. Lett. **103**, 051101 (2009) [arXiv:0810.2784 [astro-ph]];
S. Profumo, arXiv:0812.4457 [astro-ph];
D. Malyshev, I. Cholis and J. Gelfand, Phys. Rev. D **80**, 063005 (2009) [arXiv:0903.1310 [astro-ph.HE]];
V. Barger, Y. Gao, W. Y. Keung, D. Marfatia and G. Shaughnessy, Phys. Lett. B **678**, 283 (2009) [arXiv:0904.2001 [hep-ph]];
D. Grasso *et al.* [FERMI-LAT Collaboration], Astropart. Phys. **32**, 140 (2009) [arXiv:0905.0636 [astro-ph.HE]];
P. Mertsch and S. Sarkar, Phys. Rev. Lett. **103**, 081104 (2009) [arXiv:0905.3152 [astro-ph.HE]];
D. Malyshev, JCAP **0907**, 038 (2009) [arXiv:0905.2611 [astro-ph.HE]];
K. Kashiyama, K. Ioka and N. Kawanaka, arXiv:1009.1141 [astro-ph.HE].

[17] N. J. Shaviv, E. Nakar and T. Piran, Phys. Rev. Lett. **103**, 111302 (2009) [arXiv:0902.0376 [astro-ph.HE]];
Y. Fujita, K. Kohri, R. Yamazaki and K. Ioka, Phys. Rev. D **80**, 063003 (2009) [arXiv:0903.5298 [astro-ph.HE]].

[18] P. Blasi, Phys. Rev. Lett. **103**, 051104 (2009) [arXiv:0903.2794 [astro-ph.HE]];
H. B. Hu, Q. Yuan, B. Wang, C. Fan, J. L. Zhang and X. J. Bi, arXiv:0901.1520 [astro-ph];
S. Dado and A. Dar, arXiv:0903.0165 [astro-ph.HE].

[19] L. Stawarz, V. Petrosian and R. D. Blandford, Astrophys. J. **710**, 236 (2010) [arXiv:0908.1094 [astro-ph.GA]];
R. Cowsik and B. Burch, arXiv:0905.2136 [astro-ph.CO];
B. Katz, K. Blum and E. Waxman, arXiv:0907.1686 [astro-ph.HE].

[20] Y. Z. Fan, B. Zhang and J. Chang, arXiv:1008.4646 [astro-ph.HE].
[21] Y. Cui, J. D. Mason and L. Randall, arXiv:1006.0983 [hep-ph], and references therein.
[22] M. Lindner, A. Merle and V. Niro, arXiv:1005.3116 [hep-ph].
[23] M. Beltran, D. Hooper, E. W. Kolb and Z. C. Krusberg, Phys. Rev. D **80**, 043509 (2009) [arXiv:0808.3384 [hep-ph]].
[24] C. C. Nishi, Am. J. Phys. **73**, 1160 (2005) [arXiv:hep-ph/0412245].
[25] C. Itzykson and J.B. Zuber, Quantum Field Theory, pages 161-2, Dover Pr., 1980.
[26] Y. Takahashi, *"The Fierz Identities"*, in *Progress in Quantum Field Theory*, ed. H. Ezawa and S. Kamefuchi (North Holland, Amsterdam, 1986), p. 121.
[27] M. E. Peskin and D. V. Schroeder, An Introduction To Quantum Field Theory, Westview Pr., 1995.
[28] S. Weinberg, *Cambridge, UK: Univ. Pr. (1995) 609 p*
[29] M. Srednicki, Quantum Field Theory, Cambridge U. Press, 2007.
[30] H. Goldberg, Phys. Rev. Lett. **50**, 1419 (1983), making use of some earlier Fierzing by P. Fayet, Phys. Lett. B **86**, 272 (1979).
A detailed calculation of the related amplitude $e^+e^- \to \tilde{\gamma}\tilde{\gamma}$ involving two identical Majorana particles is available in App. E (as well as a lucid and complete presentation of Feynman rules for Majorana fermions in App. D) of H. E. Haber and G. L. Kane, Phys. Rept. **117**, 75 (1985). Another lucid listing of Feynman rules for Majorana fermions is available in Chapter 49 of "Quantum Field Theory", by M. Srednicki, Cambridge University Press.
[31] Q. H. Cao, E. Ma and G. Shaughnessy, Phys. Lett. B **673**, 152 (2009) [arXiv:0901.1334 [hep-ph]].
[32] E. Ma, Phys. Rev. Lett. **86**, 2502 (2001) [arXiv:hep-ph/0011121].
[33] G. B. Gelmini, E. Osoba and S. Palomares-Ruiz, Phys. Rev. D **81**, 063529 (2010) [arXiv:0912.2478 [hep-ph]].
[34] P. Ciafaloni and D. Comelli, Phys. Lett. B **446**, 278-284 (1999) [arXiv:hep-ph/9809321];
M. Beccaria, P. Ciafaloni, D. Comelli, F.M. Renard, C. Verzegnassi, Phys. Rev. D **61** 073005 (2000) [arXiv:hep-ph/9906319];
V.S. Fadin, L.N. Lipatov, Alan D. Martin, M. Melles, Phys. Rev. D **61** 094002 (2000) [arXiv:hep-ph/9910338];
W. Beenakker, A. Werthenbach, Phys. Lett. B **489** 148-156 (2000) [arXiv:hep-ph/0005316];
Michael Melles, Phys. Rept. **375** 219-326 (2003) [arXiv:hep-ph/0104232];
G. Bell, J. H. Kuhn and J. Rittinger, arXiv:1004.4117 [hep-ph];
P. Ciafaloni, D. Comelli, A. Riotto, F. Sala, A. Strumia and A. Urbano, arXiv:1009.0224 [hep-ph];
and ref. [6].
[35] L.D. Landau and E.M. Lifschitz, "The Classical Theory of Fields", Pergamon Press, 4^{th} revised Enlish edition, pages 32-34.
[36] P. Gondolo and G. Gelmini, Nucl. Phys. B360, 145 (1991).
[37] Some may recognize the logarithmic factor in Eq. (23) as twice the rapidity of the produced W, i.e. $y_W = \frac{1}{2}\ln(\frac{E_W+p_W}{E_W-p_W})$.
[38] R. M. Crocker, N. F. Bell, C. Balazs and D. I. Jones, Phys. Rev. D **81**, 063516 (2010) [arXiv:1002.0229 [hep-ph]].
[39] S. Schael *et al.* [ALEPH Collaboration], Phys. Lett. B **639**, 192 (2006) [arXiv:hep-ex/0604023].
[40] N. F. Bell, J. B. Dent, T. D. Jacques and T. J. Weiler, in preparation.
[41] Summary Tables from the Particle Data Group, http://pdg.lbl.gov/